

Multi-View Representation Learning: A Survey from Shallow Methods to Deep Methods

Yingming Li, Ming Yang, Zhongfei (Mark) Zhang, *Senior Member, IEEE*

Abstract—Recently, multi-view representation learning has become a rapidly growing direction in machine learning and data mining areas. This paper introduces several principles for multi-view representation learning: correlation, consensus, and complementarity principles. Consequently, we first review the representative methods and theories of multi-view representation learning based on correlation principle, especially on canonical correlation analysis (CCA) and its several extensions. Then from the viewpoint of consensus and complementarity principles we investigate the advancement of multi-view representation learning that ranges from shallow methods including multi-modal topic learning, multi-view sparse coding, and multi-view latent space Markov networks, to deep methods including multi-modal restricted Boltzmann machines, multi-modal autoencoders, and multi-modal recurrent neural networks. Further, we also provide an important perspective from manifold alignment for multi-view representation learning. Overall, this survey aims to provide an insightful overview of theoretical basis and state-of-the-art developments in the field of multi-view representation learning and to help researchers find the most appropriate tools for particular applications.

Index Terms—Multi-view representation learning, canonical correlation analysis, multi-modal deep learning.

1 INTRODUCTION

Multi-view data have become increasingly available in real-world applications where examples are described by different feature sets or different “views”, such as image+text, audio+video, and webpage+click-through data. The different views usually contain complementary information, and multi-view learning can exploit this information to learn representation that is more expressive than that of single-view learning methods. Therefore, multi-view representation learning has become a very promising topic with wide applicability.

Canonical correlation analysis (CCA) [1] and its kernel extensions [2–4] are representative techniques in early studies of multi-view representation learning. A variety of theories and approaches are later introduced to investigate their theoretical properties, explain their success, and extend them to improve the generalization performance in particular tasks. While CCA and its kernel versions show their abilities of effectively modeling the relationship between two or more sets of variables, they have limitations on capturing high level associations between multi-view data. Inspired by the success of deep neural networks [5–7], deep CCAs [8] have been proposed to solve this problem, with a common strategy to learn a joint representation that is coupled between multiple views at a higher level after learning several layers of view-specific features in the lower layers. However, how to learn a good association between multi-view data still remains an open problem. In 2016, a workshop on multi-view representation learning is held in conjunction with the 33rd international conference on machine learning to help promote a better understanding of various approaches and the challenges in specific applications. So far, there have been increasing research activities in this direction and a large number of multi-view representation

learning algorithms have been presented based on the fundamental theories of CCAs and progress of deep neural networks. For example, the advancement of multi-view representation learning ranges from shallow methods including multi-modal topic learning [9–11], multi-view sparse coding [12–14], and multi-view latent space Markov networks [15, 16], to deep methods including multi-modal deep Boltzmann machines [17], multi-modal deep autoencoders [18–20], and multi-modal recurrent neural networks [21–23]. Further, manifold alignment also provides an important perspective for multi-view representation learning [24].

Therefore, we first introduce several principles for multi-view representation learning: (i) correlation principle, it aims to maximize the correlations among variables between multiple different views; (ii) consensus principle, it seeks to maximize the agreement on the representations learned from multiple different views; (iii) complementarity principles, this principle seeks to exploit the complementary knowledge contained in multiple views to comprehensively represent the data. Most of the literature has utilized these principles in one way or another, even though in many cases the relationship between the proposed frameworks and these underlying principles are not made as an in-depth discussion.

Consequently, we review the literature of multi-view representation learning from shallow methods to deep methods in accordance with its progress and underlying common principles. In particular, each part is surveyed by the following two broad, parallel lines of this learning mechanism: one rooted in probabilistic graphical models and the other rooted in non-linear embedding models including the kernel trick and neural networks. In fact, the fundamental difference between the two paradigms is whether the layered architecture of a learning model is to be interpreted as a probabilistic graphical model or as a computation network. The connection between these two paradigms becomes more obvious when we consider deeper multi-view representation learning models. The computational networks have become increasingly important for big data learning since the exact inference of probabilistic models usually becomes intractable with deep

• *Y. Li, M. Yang, Z. Zhang are with College of Information Science & Electronic Engineering, Zhejiang University, China.
E-mail: {yingming, cauchym, zhongfei}@zju.edu.cn*

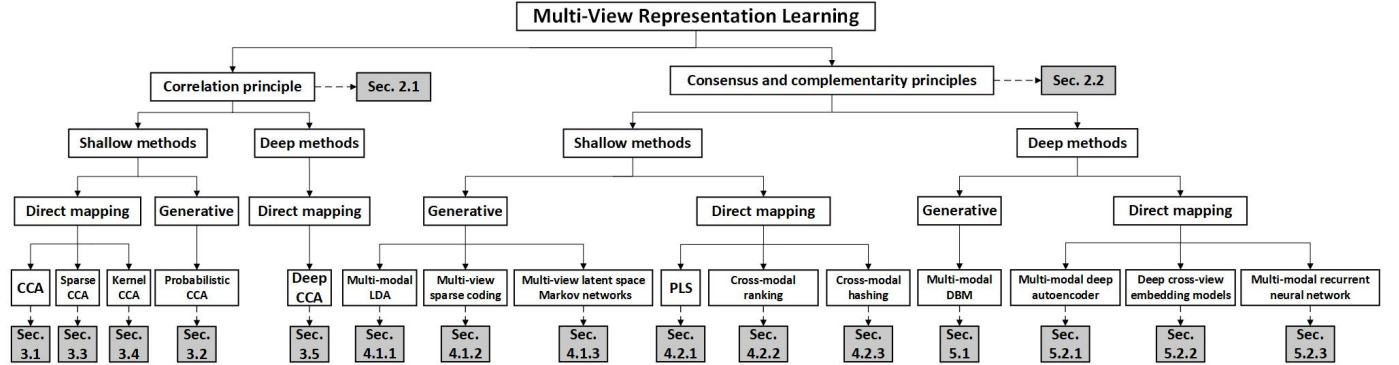


Fig. 1. The basic organization of this survey. The left part shows the architecture of multi-view representation learning methods based on correlation principle, and the right part displays the structure of multi-view embedding models based on consensus and complementarity principles.

structures.

The goal of this survey is to review the theoretical basis and key advances in the area of multi-view representation learning and to provide a global picture of this active direction. We expect this survey to help researchers find the most appropriate approaches for their particular applications and deliver perspectives of what can be done in the future to promote the development of multi-view representation learning.

1.1 Organization of This Survey

Figure 1 illustrates the organization of this survey, which is based on several underlying principles which ensure the success of multi-view representation learning: correlation, consensus, and complementarity principles. The correlation principle focuses on maximizing the correlations between multi-view embeddings and the representative examples are CCA and its extensions. Both consensus and complementarity principles play important roles in multi-view representation learning. A great number of multi-view embedding models are proposed by considering the consistency and complementarity of different views simultaneously. Taking multi-view latent space modeling [11, 15] for example, consensus principle is responsible for achieving agreement in a shared low-dimensional representation and complementarity principle guarantees the integration of the complementary knowledge underlying different views.

Inspired by the success of deep neural networks [5, 6, 25], a variety of deep multi-view embedding methods have been proposed to learn robust multi-view representation. Consequently, as shown in Figure 1, we categorize the learning models into shallow and deep methods and then discuss in detail the representative models from generative and direct mapping mechanisms. Moreover, in Section 6 we also investigate manifold alignment learning, where multi-view representation learning can be considered as finding the consistent relationship among structures of manifolds from the multiple views.

1.2 Main Differences from Other Related Surveys

Recently, several related surveys [4, 26–29] of multi-view learning have been introduced to investigate the theories and applications of the existing multi-view learning algorithms. Among them, the closest efforts to this article are [4] and [28]. Both of them focus on multi-view learning techniques using the traditional feature

learning methods, and give a comprehensive overview of multi-view learning.

The main differences between these two surveys and this survey are concluded as follows. First, this survey focuses on the multi-view representation learning, while the other two surveys concern all the aspects of multi-view learning. Second, this survey provides a more detailed analysis of various multi-view representation learning models from shallow literature to deep frameworks. In comparison, the other two surveys mainly investigate the shallow multi-view embedding methods and ignore the recent developments of deep methods. Third, [28] classifies the multi-view learning algorithms into three different settings: co-training style, multiple kernel learning, and subspace learning; the survey of [4] provides a comprehensive review of CCA, effectiveness of co-training, and generalization error analysis for co-training and other multi-view learning approaches. In contrast to these two surveys, this survey is formulated as a general embedding-based architecture from shallow aspects to deep counterparts that helps understand the key idea of multi-view representation learning. For example, this survey investigates a great number of deep multi-view embedding models which exploit deep visual and linguistic features, while the other surveys focus on the traditional feature extraction methods for multi-view learning.

2 PRINCIPLES FOR MULTI-VIEW REPRESENTATION LEARNING

In contrast to single-view representation learning, multi-view representation learning introduces one embedding for modeling a particular view and jointly optimizes all the embeddings to leverage the abundant information from multi-views and boost the performance of subsequent learning tasks, such as classification and object recognition. However, if the learning scenario is not able to coincide with the statistical properties of multi-view data, the obtained representation may even reduce the learning performance. Through fully investigating the characteristics of the existing successful multi-view representation learning techniques, we observe that there are several common underlying principles behind their success: *correlation, consensus, and complementarity* principles.

2.1 Correlation Principle

Correlation principle aims to maximize the correlations of variables among multiple different views. Given a pair of datasets

$X = [x_1, \dots, x_n]$ and $Y = [y_1, \dots, y_n]$, Hotelling [1] proposes Canonical Correlation Analysis to find linear projections w_x and w_y , which make the corresponding examples in the two datasets maximally correlated in the projected space,

$$\rho = \max_{w_x, w_y} \text{corr}(w_x^\top X, w_y^\top Y) \quad (1)$$

where $\text{corr}(\cdot)$ denotes the sample correlation function between $w_x^\top X$ and $w_y^\top Y$. Thus by maximizing the correlations between the projections of the examples, the basis vectors can be computed for the two sets of variables and applied to two-view data to obtain the shared latent embedding. Since CCA is a linear multi-view representation learning algorithm, it is difficult to capture the properties of the datasets exhibiting non-linearities. Kernelization of CCA (KCCA) provides a way to cope with the non-linearities by mapping the original data to a higher-dimensional feature space. In particular, it exploits nonlinear mappings $f(X)$ and $g(Y)$, where f and g belong to reproducing kernel Hilbert spaces (RKHS) \mathcal{H}_x and \mathcal{H}_y respectively, such that its objective can be formulated as follows:

$$\max_{\substack{f \in \mathcal{H}_x, g \in \mathcal{H}_y \\ f \neq 0, g \neq 0}} \text{corr}(f(X), g(Y)) \quad (2)$$

As a non-linear extension of CCA, kernel CCA has been successfully applied in many situations, including independent component analysis [2] and cross-media learning [3]. With the growing interest in learning sparse representation of multi-view data, the problem of sparse CCA [30] has attracted much attention and can be considered as learning projections w_x and w_y with sparsity constraint which maximizes the correlation,

$$\begin{aligned} \rho &= \max_{w_x, w_y} \text{corr}(w_x^\top X, w_y^\top Y) \\ \text{s.t.} \quad & \|w_x\|_0 \leq s_x, \quad \|w_y\|_0 \leq s_y. \end{aligned} \quad (3)$$

Further, the correlation principle can be naturally applied to multi-view neural network learning to learn deep and abstract multi-view representations. For example, deep CCA is proposed by Andrew et al. [8] to obtain deep nonlinear mappings between two views $\{X, Y\}$ which are maximally correlated. Consequently, a deep canonically correlated autoencoder (DCCAE) [20] is introduced through jointly optimizing the objectives of the deep CCA and the separate autoencoders from multiple views.

2.2 Consensus and Complementarity Principles

In this section, we first introduce the respective characteristics of consensus and complementarity principles, and then review multi-view embedding methods which succeeds by combining them together to take advantage of each principle.

2.2.1 Consensus principle

Consensus principle seeks to maximize the agreement on the representations learned from multiple different views. Suppose we have the two-view given dataset X and Y . Let $f(x; W_f)$ and $g(y; W_g)$ denote the embeddings from the inputs to the learned representations, respectively, where $\theta = \{W_f, W_g\}$ indicates the corresponding parameters. A natural agreement measure between the i -th pair representation of x_i and y_i can be formulated as follows:

$$\min_{\theta} \|f(x_i; W_f) - g(y_i; W_g)\|_2^2 \quad (4)$$

where the loss function enforces the consistency between two distinct views' representation. By extending this consistency constraint, various multi-view representation learning methods are proposed in decades. For example, Cross-modal factor analysis (CFA) is introduced by Li et al. [31] as a simple example of multi-view embedding learning based on the consensus principle. For a given pair (x_i, y_i) , it aims at finding orthogonal transformation matrices W_x and W_y that minimize the following expression:

$$\|x_i^\top W_x - y_i^\top W_y\|_2^2 + r_x(W_x) + r_y(W_y) \quad (5)$$

where $r_x(\cdot)$ and $r_y(\cdot)$ are regularization terms.

Besides, consensus principle is also applied in multi-view deep representation learning. Correspondence autoencoder [19] imposes a consistency constraint on selected code layers to build correspondence between two views' representations and its loss function on any pair of inputs is defined as follows:

$$\begin{aligned} L &= \lambda_y \|x_i - \hat{x}_i\|_2^2 + \lambda_y \|y_i - \hat{y}_i\|_2^2 \\ &\quad + \|f^c(x_i; W_f) - g^c(y_i; W_g)\|_2^2 \end{aligned} \quad (6)$$

where $f^c(x_i; W_f)$ and $g^c(y_i; W_g)$ denote the specific corresponding code layers.

2.2.2 Complementarity principle

The complementarity principle demonstrates that in multi-view representation learning, multiple views provide complementary information. Consequently, multiple views can be integrated into a single multi-view representation which captures the underlying concept that the data correspond to. A complementarity principle seeks to maximize the impact of the complementary knowledge contained in multiple views to comprehensively represent the data.

Thus, this complementarity principle has been utilized in a great number of multi-view representation learning methods by different ways. One traditional way is to construct multi-view representations by concatenating representation vectors from different views. For example, Kiela and Bottou [33] obtain multi-modal concept representations by concatenating a skip-gram linguistic representation vector with a visual concept representation learned with a deep convolution neural network. This complementarity learning method has shown its advantage on tasks of semantic relatedness. Collell et al. [34] build multi-view representation by using visual predictions from a learned language-to-vision mapping.

Further, Karpathy and Li [21] introduce a multi-modal recurrent neural network to generate image descriptions. This approach learns multi-modal embeddings for language and visual data and then exploits their complementary information to predict a variable-sized text given an image. Inspired by the success of attention mechanism in machine translation, Xu et al. [35] propose an attention based multi-modal recurrent neural network that automatically learns to describe the content of images. Similarly, through multi-modal embedding the complementary knowledge underlying text and image data can be unified to improve the prediction performance by using the complementarity principle.

2.2.3 Combination of Consensus and Complementarity Principles

Both consensus and complementarity principles play important roles in multi-view representation learning. A great number of multi-view embedding models are proposed by considering the

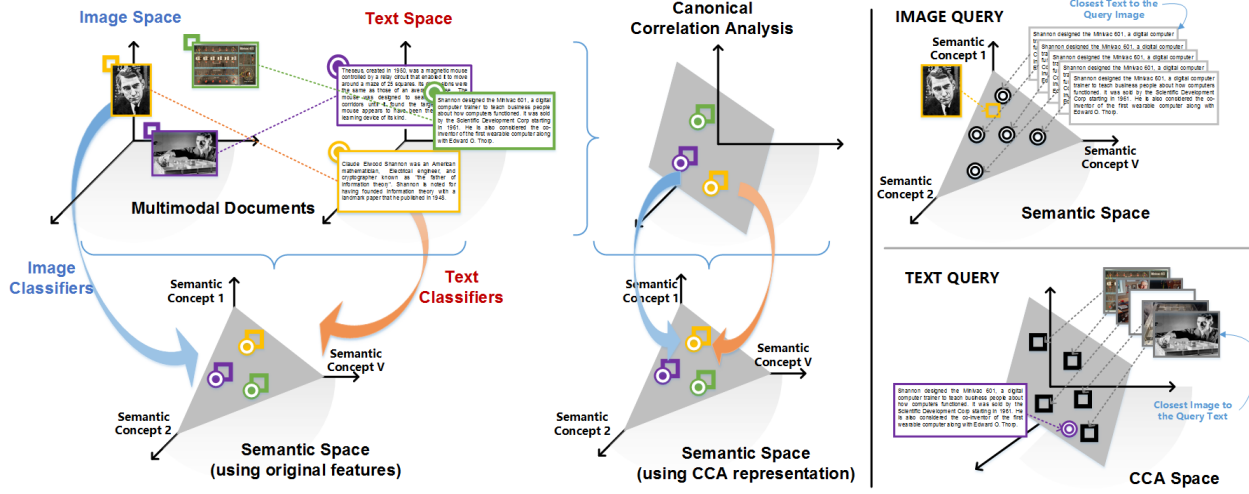


Fig. 2. An illustrative example application of CCA in cross-modal retrieval (adapted from [32]). Left: Embedding of the text and image from their source spaces to a CCA space, Semantic Space and a Semantic space learned using CCA representation. Right: examples of cross-modal retrieval where both text and images are mapped to a common space. At the top is shown an example of retrieving text in response to an image query with a common semantic space. At the bottom is shown an example of retrieving images in response to a text query with a common subspace using CCA.

consistency and complementarity of different views simultaneously, such as multi-modal topic learning [11], multi-view sparse coding [12], multi-view latent space Markov networks [15, 16], and multi-modal deep Boltzmann machines [17].

Further, taking collective matrix factorization (CMF) [36–38] for example, it learns shared multi-view representations over the joint space of multi-view data by fully considering both consensus and complementarity principles. In particular, a simple form of CMF considers multiple views' data matrices $\{X_i \in \mathbb{R}^{n \times d_i}\}_{i \in \mathcal{I}}$ of the same row dimensionality, and simultaneously factorizes them based on the following form

$$X_i = UV_i^\top \text{ for all } i \in \mathcal{I} \quad (7)$$

where it is assumed that these data matrices from multiple views share the same lower-dimensional factor matrix $U \in \mathbb{R}^{n \times k}$ which can be considered as the common representation across different views and each data matrix has its own loading matrix $V_i \in d_i \times k$. Bias for different factors and loadings can also be incorporated [39].

To use CMF, we must compute the factors and loadings given multiple observed data matrices. The common approach is to minimize the regularized squared error loss with respect to U and $\{V_i\}_{i \in \mathcal{I}}$,

$$\min_{U, V_i} \sum_{i \in \mathcal{I}} \lambda_{X_i} \|X_i - UV_i^\top\|_F^2 + \lambda_U \|U\|_F^2 + \sum_{i \in \mathcal{I}} \lambda_{V_i} \|V_i\|_F^2 \quad (8)$$

where λ_U and λ_{V_i} are regularization parameters.

From the above objective in Eq.(8), we can see that the shared representation matrix U is generated by combining data matrices across views, where the consensus ensures the mutual agreement on multiple views of data and the complementarity exploits the distinctive information contained in different views for learning the complete representation which is useful for classification and retrieval.

3 CANONICAL CORRELATION ANALYSIS AND ITS EXTENSIONS

In this section we will review the multi-view representation learning techniques based on the correlation principle: canonical correlation analysis (CCA) and its extensions that range from shallow modeling to non-linear deep embedding. In particular, we will investigate the related work of probabilistic CCA, sparse CCA, kernel CCA and deep CCA to illustrate the direct mapping and generative views of multi-view representation learning theories.

3.1 Canonical Correlation Analysis

Canonical Correlation Analysis [1] has become increasingly popular for its capability of effectively modeling the relationship between two or more sets of variables. From the perspective of multi-view representation learning, CCA computes a shared embedding of both sets of variables through maximizing the correlations among the variables between the two sets. More specifically, CCA has been widely used in multi-view learning tasks to generate low-dimensional representations [32, 40, 41]. Improved generalization performance has been witnessed in areas including dimensionality reduction [42–44], clustering [45–47], regression [48, 49], word embeddings [50–52], and discriminant learning [53–55]. For example, Figure 2 shows a fascinating cross-modality application of CCA in cross-media retrieval.

Given a pair of datasets $X = [x_1, \dots, x_n]$ and $Y = [y_1, \dots, y_n]$, CCA tends to find linear projections w_x and w_y , which make the corresponding examples in the two datasets maximally correlated in the projected space. The correlation coefficient between the two datasets in the projected space is given by

$$\rho = \text{corr}(w_x^\top X, w_y^\top Y) = \frac{w_x^\top C_{xy} w_y}{\sqrt{(w_x^\top C_{xx} w_x)(w_y^\top C_{yy} w_y)}} \quad (9)$$

where the covariance matrix C_{xy} is defined as

$$C_{xy} = \frac{1}{n} \sum_{i=1}^n (x_i - \mu_x)(y_i - \mu_y)^\top \quad (10)$$

where $\mu_x = \frac{1}{n} \sum_{i=1}^n x_i$ and $\mu_y = \frac{1}{n} \sum_{i=1}^n y_i$ are the means of the two views, respectively. The definition of C_{xx} and C_{yy} can be obtained similarly.

Since the correlation ρ is invariant to the scaling of w_x and w_y , CCA can be posed equivalently as a constrained optimization problem.

$$\begin{aligned} & \max_{w_x, w_y} w_x^T C_{xy} w_y \\ \text{s.t. } & w_x^T C_{xx} w_x = 1, \quad w_y^T C_{yy} w_y = 1 \end{aligned} \quad (11)$$

By formulating the Lagrangian dual of Eq.(11), it can be shown that the solution to Eq.(11) is equivalent to solving a pair of generalized eigenvalue problems [3],

$$\begin{aligned} C_{xy} C_{yy}^{-1} C_{yx} w_x &= \lambda^2 C_{xx} w_x \\ C_{yx} C_{xx}^{-1} C_{xy} w_y &= \lambda^2 C_{yy} w_y \end{aligned} \quad (12)$$

Besides the above definition of CCA, there are also other different ways to define the canonical correlations of a pair of matrices, and all these ways are shown to be equivalent [56]. In particular, Kettenring [57] shows that CCA is equivalent to a constrained least-square optimization problem. Further, Golub and Zha [56] also provide a classical algorithm for computing CCA by first QR decomposition of the data matrices which whitens the data and then an SVD of the whitened covariance matrix. However, with typically huge data matrices this procedure becomes extremely slow. Avron et al. [44, 58] propose a fast algorithm for CCA with a pair of tall-and-thin matrices using subsampled randomized Walsh-Hadamard transform [59], which only subsamples a small proportion of the training data points to approximate the matrix product. Further, Lu and Foster [60] consider sparse design matrices and introduce an efficient iterative regression algorithm for large scale CCA.

Another line of research for large scale CCA considers stochastic optimization algorithm for CCA [61]. Ma et al. [62] introduce an augmented approximate gradient scheme and further extend it to a stochastic optimization regime. Recent work [63, 64] attempts to transform the original problem of CCA into sequences of least squares problems and solve these problems with accelerated gradient descent (AGD). Further, Sun et al. [41] formulate CCA as a least squares problem in multi-label classification.

While CCA has the capability of conducting multi-view feature learning and has been widely applied in different fields, it still has some limitations in different applications. For example, it ignores the nonlinearities of multi-view data. Consequently, many algorithms based on CCA have been proposed to extend the original CCA in real-world applications. In the following sections, we review its several widely-used extensions including probabilistic CCA, sparse CCA, kernel CCA and Deep CCA.

3.2 Probabilistic CCA

CCA can be interpreted as the maximum likelihood solution to a probabilistic latent variable model for two Gaussian random vectors. This formulation of CCA as a probabilistic model is proposed by Bach and Jordan [65].

Probabilistic CCA can be formulated by first introducing an explicit latent variable z corresponding to the principal-component subspace. And then a Gaussian prior distribution $p(z)$ is assumed over the latent variable, together with two Gaussian conditional distributions $p(x|z)$ and $p(y|z)$ for the observed variables x and y conditioned on the value of the latent variable. In particular, the

prior distribution over z is given by a zero-mean unit-covariance Gaussian

$$p(z) = \mathcal{N}(z|0, I_M) \quad (13)$$

Similarly, the conditional distributions of the observed variable x and y , conditioned on the value of the latent variable z , are also Gaussian and given as follows,

$$\begin{aligned} p(x|z) &= \mathcal{N}(x|W_x z + \mu_x, \Psi_x) \\ p(y|z) &= \mathcal{N}(y|W_y z + \mu_y, \Psi_y) \end{aligned} \quad (14)$$

where the means of x and y are in general linear functions of z governed by the $d_x \times d_z$ matrix W_x and the d_x -dimensional vector μ_x , and by the $d_y \times d_z$ matrix W_y and the d_y -dimensional vector μ_y , respectively. The crucial idea lies in that the latent variable z is shared by the two data sets, while other variables or parameters are independent.

Consequently, Bach and Jordan [65] provide a detailed connection between CCA and probabilistic CCA based on the result of the maximum likelihood estimation of Eq.(14) that $W_x = \Sigma_{xx} U_x P^{1/2} R$ and $W_y = \Sigma_{yy} U_y P^{1/2} R$, where U is composed of the canonical directions, P is a diagonal matrix containing the canonical correlations, and R is an arbitrary rotation matrix. Further, the posterior expectations $E(z|x)$ and $E(z|y)$ lie in the same subspace that the traditional CCA searches since the obtained canonical weights are the same as the ones for CCA. EM algorithm is applied to find the maximum likelihood solution and is shown to converge to the global optimum. In addition, Browne [66] also proves that the maximum likelihood solution of Eq.(14) is identical to the solution of classical CCA.

However, since probabilistic CCA is based on a Gaussian density model, outliers may lead to serious biases in the parameter estimates when using a maximum likelihood estimation method. To handle the influence of outliers, Archambeau et al. [67] introduce robust canonical correlation analysis by replacing Gaussian distributions with Student- t distributions, which constructs mixtures of robust CCA and can deal with missing data quite easily. Fyfe and Leen [68] consider a Dirichlet process method for performing a non-Bayesian probabilistic mixture CCA.

By treating the mixture case in length, Klami and Kaski [69] present a full Bayesian treatment of probabilistic canonical analyzer. Further, Wang [70] applies a hierarchical Bayesian model to probabilistic CCA and learns this model by variational approximation. By performing the Bayesian model algorithm for probabilistic CCA, the number of canonical correlations can be determined automatically and one would not encounter the issue of selecting the number of canonical correlations, which has been a well known downside for using CCA. Both [69] and [70] exploit the inverse Wishart matrix distribution as a prior for the covariance matrices $\Psi_{x(y)}$ in Eq.(14) and use the automatic relevance determination prior for the linear transformation matrices $W_{x(y)}$.

Despite the apparent superiority of Bayesian CCA for model selection, it is worth pointing out that the inference of the Bayesian CCA is difficult for high-dimensional data. Most of the practical applications of Bayesian CCA in the earlier efforts focus on relatively low-dimensional data [69, 70]. To make Bayesian CCA feasible for high-dimensional data, Huopaniemi et al. [71] propose to use multi-way analysis setup by exploiting dimensionality reduction techniques.

3.3 Sparse CCA

Recent years have witnessed a growing interest in learning sparse representations of data. Correspondingly, the problem of sparse CCA also has received much attention in the multi-view representation learning. The quest for sparsity can be motivated from several aspects. First is the ability to account for the predicted results. The big picture usually relies on a small number of crucial variables, with details to be allowed for variation. The second motivation for sparsity is regularization and stability. Reasonable regularization plays an important role in eliminating the influence of noisy data and reducing the sensitivity of CCA to a small number of observations. Further, sparse CCA can be formulated as a subset selection scheme which reduces the dimensionality of the vectors and makes possible a stable solution.

The problem of sparse CCA can be considered as finding a pair of linear combinations of w_x and w_y with prescribed cardinality which maximizes the correlation. In particular, sparse CCA can be defined as the solution to

$$\begin{aligned} \rho &= \max_{w_x, w_y} \frac{w_x^\top C_{xy} w_y}{\sqrt{w_x^\top C_{xx} w_x w_y^\top C_{yy} w_y}} \\ \text{s.t. } & \|w_x\|_0 \leq s_x, \quad \|w_y\|_0 \leq s_y. \end{aligned} \quad (15)$$

Most of the approaches to sparse CCA are based on the well known LASSO trick [72] which is a shrinkage and selection method for linear regression. By formulating CCA as two constrained simultaneous regression problems, Hardoon and Shawe-Taylor [73] propose to approximate the non-convex constraints with ∞ -norm. This is achieved by fixing each index of the optimized vector to 1 in turn and constraining the 1-norm of the remaining coefficients. Similarly, Waaijenborg et al. [74] propose to use the elastic net type regression.

In addition, Sun et al. [41] introduce a sparse CCA by formulating CCA as a least squares problem in multi-label classification and directly computing it with the Least Angle Regression algorithm (LARS) [75]. Further, this least squares formulation facilitates the incorporation of the unlabeled data into the CCA framework to capture the local geometry of the data. For example, graph laplacian [76] can be used in this framework to tackle with the unlabeled data.

In fact, the development of sparse CCA is intimately related to the advance of sparse PCA [77]. The classical solutions to generalized eigenvalue problem with sparse PCA can be easily extended to that of sparse CCA [30, 78]. Torres et al. [78] derive a sparse CCA algorithm by extending an approach for solving sparse eigenvalue problems using D.C. programming. Based on the sparse PCA algorithm in [79], Wiesel et al. [30] propose a backward greedy approach to sparse CCA by bounding the correlation at each stage. Witten et al. [80] propose to apply a penalized matrix decomposition to the covariance matrix C_{xy} , which results in a method for penalized sparse CCA. Consequently, structured sparse CCA has been proposed by extending the penalized CCA with structured sparsity inducing penalty [81].

3.4 Kernel CCA

Canonical Correlation Analysis is a linear multi-view representation learning algorithm, but for many scenarios of real-world multi-view data revealing nonlinearities, it is impossible for a linear embedding to capture all the properties of the multi-view data [28]. Since kernerlization is a principled trick for introducing non-linearity into linear methods, kernel CCA [82, 83] provides

an alternative solution. As a non-linear extension of CCA, kernel CCA has been successfully applied in many situations, including independent component analysis [2], cross-media information retrieval [3, 84, 85], computational biology [3, 86, 87], multi-view clustering [46, 88], acoustic feature learning [89, 90], and statistics [2, 91].

The key idea of kernel CCA lies in embedding the data into a higher dimensional feature space $\phi_x : \mathcal{X} \rightarrow \mathcal{H}_x$, where \mathcal{H}_x is the reproducing kernel Hilbert space (RKHS) associated with the real numbers, $k_x : \mathcal{X} \times \mathcal{X} \rightarrow \mathbb{R}$ and $k_x(x_i, x_j) = \langle \phi_x(x_i), \phi_x(x_j) \rangle$. k_y, \mathcal{H}_y , and ϕ_y can be defined analogously.

By adapting the representer theorem [92] to the case of multi-view data to state that the following minimization problem,

$$\begin{aligned} \min_{f_1, \dots, f_K} & L((x_1, y_1, f_x(x_1), f_y(y_1)), \dots, (x_n, y_n, f_x(x_n), f_y(y_n))) \\ & + \Omega_x(\|f\|_K^2, \|f\|_K^2) \end{aligned} \quad (16)$$

where L is an arbitrary loss function and Ω is a strictly monotonically increasing function, admits representation of the form

$$f_x(x) = \sum_i \alpha_i k_x(x_i, x), \quad f_y(y) = \sum_i \beta_i k_y(y_i, y) \quad (17)$$

Correspondingly, we replace vectors w_x and w_y in our previous CCA formulation Eq.(9) with $f_x = \sum_i \alpha_i \phi_x(x_i)$ and $f_y = \sum_i \beta_i \phi_y(y_i)$, respectively, and replace the covariance matrices accordingly. The kernel CCA objective can be written as follows:

$$\rho = \frac{f_x^\top \hat{C}_{xy} f_y}{\sqrt{f_x^\top \hat{C}_{xx} f_x f_y^\top \hat{C}_{yy} f_y}} \quad (18)$$

In particular, the kernel covariance matrix \hat{C}_{xy} is defined as

$$\hat{C}_{xy} = \frac{1}{n} \sum_{i=1}^n (\phi_x(x_i) - \mu_{\phi_x(x)}) (\phi_y(y_i) - \mu_{\phi_y(y)})^\top, \quad (19)$$

where $\mu_{\phi_x(x)} = \frac{1}{n} \sum_{i=1}^n \phi_x(x_i)$ and $\mu_{\phi_y(y)} = \frac{1}{n} \sum_{i=1}^n \phi_y(y_i)$ are the means of the two views' kernel mappings, respectively. The form of \hat{C}_{xx} and \hat{C}_{yy} can be obtained analogously.

Let K_x denote the kernel matrix such that $K_x = H \tilde{K}_x H$, where $[\tilde{K}_x]_{ij} = k_x(x_i, x_j)$ and $H = I - \frac{1}{n} \mathbf{1} \mathbf{1}^\top$ is a centering matrix, $\mathbf{1} \in \mathbb{R}^n$ being a vector of all ones. And K_y is defined similarly. Further, we substitute them into Eq.(18) and formulate the objective of kernel CCA as the following optimization problem:

$$\max_{\alpha, \beta} \frac{\alpha^\top K_x K_y \beta}{\sqrt{\alpha^\top K_x^2 \alpha \beta^\top K_y^2 \beta}} \quad (20)$$

As discussed in [3], the above optimization leads to degenerate solutions when either K_x or K_y is invertible. Thus, we introduce regularization terms and maximize the following regularized expression

$$\max_{\alpha, \beta} \frac{\alpha^\top K_x K_y \beta}{\sqrt{\alpha^\top (K_x^2 + \epsilon_x K_x) \alpha \beta^\top (K_y^2 + \epsilon_y K_y) \beta}} \quad (21)$$

Since this new regularized objective function is not affected by re-scaling of α or β , we assume that the optimization problem is subject to

$$\begin{aligned} \alpha^\top K_x^2 \alpha + \epsilon_x \alpha^\top K_x \alpha &= 1 \\ \beta^\top K_y^2 \beta + \epsilon_y \beta^\top K_y \beta &= 1 \end{aligned} \quad (22)$$

Similar to the optimized case of CCA, by formulating the Lagrangian dual of Eq.(21) with the constraints in Eq.(22), it can be shown that the solution to Eq.(21) is also equivalent to solving a pair of generalized eigenproblems [3],

$$\begin{aligned} (K_x + \epsilon_x I)^{-1} K_y (K_y + \epsilon_y I)^{-1} K_x \alpha &= \lambda^2 \alpha \\ (K_y + \epsilon_y I)^{-1} K_x (K_x + \epsilon_x I)^{-1} K_y \beta &= \lambda^2 \beta \end{aligned} \quad (23)$$

Consequently, the statistical properties of KCCA have been investigated from several aspects [2, 93]. Fukumizu et al. [94] introduce a mathematical proof of the statistical convergence of kernel CCA by providing rates for the regularization parameters. Later Hardoon and Shawe-Taylor [95] provide a detailed theoretical analysis of KCCA and propose a finite sample statistical analysis of KCCA by using a regression formulation. Cai and Sun [96] also provide a convergence rate analysis of kernel CCA under an approximation assumption. However, the problems of choosing appropriate regularization parameters in practice remain largely unsolved.

In addition, KCCA has a closed-form solution via the eigenvalue system in Eq.(23), but this solution does not scale up to the large size of the training set, due to the problem of time complexity and memory cost. Thus, various approximation methods have been proposed by constructing low-rank approximations of the kernel matrices, including incomplete Cholesky decomposition [2], partial Gram-Schmidt orthogonalisation [3], and block incremental SVD [89, 97]. In addition, the Nyström method [98] is widely used to speed up the kernel machines [99–102]. This approach is achieved by carrying out an eigen-decomposition on a lower-dimensional system, and then expanding the results back up to the original dimensions.

3.5 Deep CCA

The CCA-like objectives can be naturally applied to neural networks to capture high-level associations between data from multiple views. In the early work, by assuming that different parts of the perceptual input have common causes in the external world, Becker and Hinton [103] present a multilayer nonlinear extension of canonical correlation by maximizing the normalized covariation between the outputs from two neural network modules. Further, Becker [104] explores the idea of maximizing the mutual information between the outputs of different network modules to extract higher order features from coherence inputs.

Later Lai and Fyfe [105, 106] investigate a neural network implementation of CCA and maximize the correlation (rather than canonical correlation) between the outputs of the networks for different views. Hsieh [107] formulates a nonlinear canonical correlation analysis (NLCCA) method using three feedforward neural networks. The first network maximizes the correlation between the canonical variates (the two output neurons), while the remaining two networks map the canonical variates back to the original two sets of variables.

Although multiple CCA-based neural network models have been proposed for decades, the full deep neural network extension of CCA, referred as deep CCA, has recently been developed by Andrew et al. [8]. Inspired by the recent success of deep neural networks [6, 25], Andrew et al. [8] introduce deep CCA to learn deep nonlinear mappings between two views $\{X, Y\}$ which are maximally correlated. The deep CCA learns representations of the two views by using multiple stacked layers of nonlinear mappings. In particular, assume for simplicity that

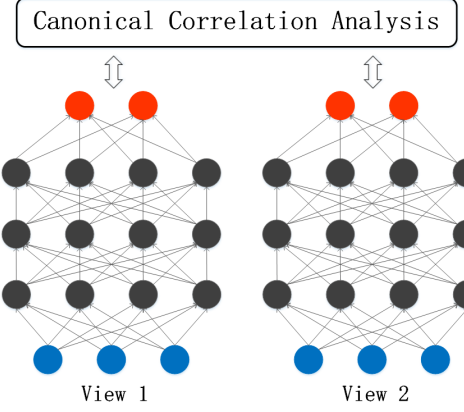


Fig. 3. The framework of deep CCA (adapted from [8]), in which the output layers of two deep networks are maximally correlated.

a network has d intermediate layers, deep CCA first learns deep representation from $f_x(x) = h_{W_x, b_x}(x)$ with parameters $(W_x, b_x) = (W_x^1, b_x^1, W_x^2, b_x^2, \dots, W_x^d, b_x^d)$, where $W_x^l(ij)$ denotes the parameters associated with the connection between unit i in layer l , and unit j in layer $l+1$. Also, $b_x^l(j)$ denotes the bias associated with unit j in layer $l+1$. Given a sample of the second view, the representation $f_y(y)$ is computed in the same way, with different parameters (W_y, b_y) . The goal of deep CCA is to jointly learn parameters for both views such that $\text{corr}(f_x(X), f_y(Y))$ is as high as possible. Let θ_x be the vector of all the parameters (W^x, b^x) of the first view and similarly for θ_y , then

$$(\theta_x^*, \theta_y^*) = \arg \max_{(\theta_x, \theta_y)} \text{corr}(f_x(X; \theta_x), f_y(Y; \theta_y)). \quad (24)$$

For training deep neural network models, parameters are typically estimated with gradient-based optimization methods. Thus, the parameters (θ_x^*, θ_y^*) are also estimated on the training data by following the gradient of the correlation objective, with batch-based algorithms like L-BFGS as in [8] or stochastic optimization with mini-batches [108–110].

Deep CCA and its extensions have been widely applied in learning representation tasks in which multiple views of data are provided. Yan and Mikolajczyk [111] learn a joint latent space for matching images and captions with a deep CCA framework, which adopts a GPU implementation and could deal with overfitting. To exploit multilingual context when learning word embeddings, Lu et al. [109] learn deep non-linear embeddings of two languages using the deep CCA.

Recently, a deep canonically correlated autoencoder (DCCAE) [20] is proposed by combining the advantages of the deep CCA and autoencoder-based approaches. In particular, DCCAE consists of two autoencoders and optimizes the combination of canonical correlation between the learned bottleneck representations and the reconstruction errors of the autoencoders. This optimization offers a trade-off between information captured in the embedding within each view on one aspect, and the information in the relationship across views on the other.

4 SHALLOW METHODS ON MULTI-VIEW REPRESENTATION LEARNING

In this section, we will investigate shallow multi-view embedding methods based on consensus and complementarity principles. In

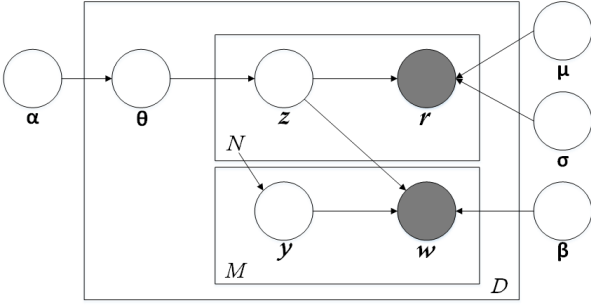


Fig. 4. The graphical model representation of the Corr-LDA model (adapted from [11]).

particular, we first review the shallow multi-view representation learning methods from probabilistic modeling perspective, and then survey the related methods from directly parameterized representation learning perspective.

4.1 Probabilistic Models

From the probabilistic modeling perspective, the problem of multi-view feature learning can be interpreted as an attempt to recover a compact set of latent random variables that describe a distribution over the observed multi-view data. We can express $p(x, y, z)$ as a probabilistic model over the joint space of the latent variables z , and the observed two-view data x, y . Feature values are determined by the posterior probability $p(z|x, y)$. Parameters are usually estimated by maximizing the regularized likelihood of the training data.

4.1.1 Multi-Modal Latent Dirichlet Allocation

Latent Dirichlet allocation (LDA) [112] is a generative probabilistic model for collections of a corpus. It proceeds beyond PLSA through providing a generative model at words and document level simultaneously. In particular, LDA is a three-level hierarchical Bayesian network that models each document as a finite mixture over an underlying set of topics.

As a generative model, LDA is extendable to multi-view data. Barnard et al. [10] present a mixture of multi-modal LDA model (MoM-LDA), which describes the following generative process for the multi-modal data: each document (consisting of visual and textual information) has a distribution for a fixed number of topics (mixture components), and given a specific topic the visual features and textual words are generated. Further, the probability distribution of the topics is different for each image-caption pair, which is achieved by imposing a Dirichlet prior for the distribution of topics.

Consequently, Blei and Jordan [11] propose a correspondence LDA (Corr-LDA) model, which not only allows simultaneous dimensionality reduction in the representation of region descriptions and words, but also models the conditional correspondence between their respectively reduced representations. The graphical model of Corr-LDA is depicted in Figure 4. This model can be viewed in terms of a generative process that first generates the region descriptions and subsequently generates the caption words.

In particular, let $\mathbf{z} = \{z_1, z_2, \dots, z_N\}$ be the latent variables that generate the image, and let $\mathbf{y} = \{y_1, y_2, \dots, y_M\}$ be discrete indexing variables that take values from 1 to N with an equal probability. Each image and its corresponding caption are

represented as a pair (\mathbf{r}, \mathbf{w}) . The first element $\mathbf{r} = \{r_1, \dots, r_N\}$ is a collection of N feature vectors associated with the regions of the image. The second element $\mathbf{w} = \{w_1, \dots, w_M\}$ is the collection of M words of the caption. Given N and M , a K -factor Corr-LDA model assumes the following generative process for an image/caption (\mathbf{r}, \mathbf{w}) :

- 1) Sample $\theta \sim \text{Dir}(\theta|\alpha)$.
- 2) For each image region $r_n, n \in \{1, \dots, N\}$:
 - a) Sample $z_n \sim \text{Mult}(\theta)$
 - b) Sample $r_n \sim p(r|z_n, \mu, \sigma)$ from a multivariate Gaussian distribution conditioned on z_n .
- 3) For each caption word $w_m, m \in \{1, \dots, M\}$:
 - a) Sample $y_m \sim \text{Unif}(1, \dots, N)$
 - b) Sample $w_m \sim p(w|y_m, \mathbf{z}, \beta)$ from a multinomial distribution conditioned on the z_{y_m} factor.

Consequently, Corr-LDA specifies the following joint distribution on image regions, caption words, and latent variables:

$$p(\mathbf{r}, \mathbf{w}, \theta, \mathbf{z}, \mathbf{y}) = p(\theta|\alpha) \left(\prod_{n=1}^N p(z_n|\theta) p(r_n|z_n, \mu, \sigma) \right) \cdot \left(\prod_{m=1}^M p(y_m|N) p(w_m|y_m, \mathbf{z}, \beta) \right) \quad (25)$$

Note that exact probabilistic inference for Corr-LDA is intractable and we employ variational inference methods to approximate the posterior distribution over the latent variables given a particular image/caption.

Following the supervised LDA algorithms [113], supervised multi-modal LDA models are subsequently proposed to make effective use of the discriminative information. Since supervised topic models can be classified into two categories: *downstream models* and *upstream models* [113], supervised multi-modal LDA models can also be categorized accordingly. For a downstream supervised multimodal model, the supervised response variables are generated from topic assignment variables. For instance, Wang et al. [114] develop a multi-modal probabilistic model for jointly modeling the image, its class label, and its annotations, called multi-class supervised LDA with annotations, which treats the class label as a global description of the image, and treats the annotation terms as local descriptions of parts of the image. Its underlying assumptions naturally integrate the multi-modal data with their discriminative information so that it takes advantage of the merits of Corr-LDA and supervised LDA [115] simultaneously.

For an upstream supervised multi-modal model, the response variables directly or indirectly generate latent topic variables [116–118]. For instance, Cao et al. [117] propose a spatially coherent latent topic model (Spatial-LTM), which represents an image containing objects in two different modalities: appearance features and salient image patches. Further, a supervised spatial-LTM model is presented by incorporating label information into distribution of topics. Nguyen et al. [119] propose a Multi-modal Multi-instance Multi-Label LDA model (M3LDA), in which the model consists of a visual-label part, a textual-label part, and a label-topic part. The underlying idea is to make the topic decided by the visual information to be consistent with the topic decided by the textual information, leading to the correct label assignment.

4.1.2 Multi-View Sparse Coding

Multi-view sparse coding [12–14] relates a latent representation (either a vector of random variables or a feature vector, depending on the interpretation) to the multi-view data through a set of linear mappings, which we refer to as the *dictionaries*. It has the property of finding shared representation h^* which picks out the most appropriate bases and zeros others, given a high degree of correlation with the input. This property is owing to the explaining away effect which arises naturally in directed graphical models [120].

Given a pair of datasets $\{X, Y\}$, a non-probabilistic multi-view sparse coding scheme can be seen as recovering the code or feature vector associated with a new multi-view input via:

$$h^* = \arg \min_h \|x - W_x h\|_2^2 + \|y - W_y h\|_2^2 + \lambda \|h\|_1 \quad (26)$$

Learning the pair of dictionaries $\{W_x, W_y\}$ can be accomplished by optimizing the following training criterion with respect to W_x and W_y :

$$\mathcal{J}_{W_x, W_y} = \sum_i (\|x_i - W_x h_i^*\|_2^2 + \|y_i - W_y h_i^*\|_2^2) \quad (27)$$

where x_i and y_i are the two modal inputs and h^* is the corresponding sparse code determined by Eq.(26). In particular, W_x and W_y are usually constrained to have unit-norm columns.

The above regularized form of multi-view sparse coding can be generalized as a probabilistic model. In probabilistic multi-view sparse coding, we assume the following generative distributions,

$$p(h) = \prod_j^d \frac{\lambda}{2} \exp(-\lambda|h_j|)$$

$$\forall_{i=1}^n : \quad p(x_i|h) = \mathcal{N}(x_i; W_x h + \mu_{x_i}, \sigma_{x_i}^2 \mathbf{I})$$

$$p(y_i|h) = \mathcal{N}(y_i; W_y h + \mu_{y_i}, \sigma_{y_i}^2 \mathbf{I}) \quad (28)$$

In the case of two-view sparse coding, because we seek a sparse multi-view representation (i.e., one with many features set to zero), we are interested in recovering the MAP (maximum *a posteriori*) value of h : i.e., $h^* = \arg \max_h p(h|x, y)$ rather than its expected value $E[h|x, y]$. Under this interpretation, learning dictionaries W_x and W_y proceeds as maximizing the likelihood of the data given these MAP values of h^* : $\arg \max_{W_x, W_y} \prod_i p(x_i|h^*)p(y_i|h^*)$ subject to the norm constraint on W_x and W_y . Note that this parameter learning scheme, subject to the MAP values of the latent h , is not a standard practice in the probabilistic graphical model literature.

Typically, the likelihood of the multi-view data is maximized directly. In the presence of latent variables, expectation maximization is employed where the parameters are optimized with respect to the marginal likelihood, i.e., summing or integrating the joint log-likelihood over the all values of the latent variables under their posterior, rather than considering only the single MAP value of h . The theoretical properties of this form of parameter learning are not yet well understood but seem to work in practice (e.g., Gaussian mixture models).

One might expect that multi-view sparse representation would significantly leverage the performance especially when features for different views are complementary to one another and indeed it seems to be the case. There are numerous examples of its successful applications as a multi-view feature learning scheme, including human pose estimation [12], image classification [121], web data mining [122], as well as cross-media retrieval [123, 124].

4.1.3 Multi-View Latent Space Markov Networks

Undirected graphical models, also called Markov random fields that have many special cases, including the exponential family Harmonium [125] and restricted Boltzmann machine [126]. Within the context of unsupervised multi-view feature learning, Xing et al. [15] first introduce a particular form of multi-view latent space Markov network model called multi-wing harmonium model. This model can be viewed as an undirected counterpart of the aforementioned directed aspect models such as multi-modal LDA [11], with the advantages that inference is fast due to the conditional independence of the hidden units and that topic mixing can be achieved by document- and feature-specific combination of aspects.

For simplicity, we begin with dual-wing harmonium model, which consists of two modalities of input units $X = \{x_i\}_{i=1}^n$, $Y = \{y_j\}_{j=1}^m$, and a set of hidden units $H = \{h_k\}_{k=1}^p$. In this dual-wing harmonium, each modality of input units and the hidden units constructs a complete bipartite graph where units in the same set have no connections but are fully connected to units in the other set. In addition, there are no connections between two input modalities. In particular, consider all the cases where all the observed and hidden variables are from exponential family; we have

$$p(x_i) = \exp\{\theta_i^T \phi(x_i) - A(\theta_i)\}$$

$$p(y_j) = \exp\{\eta_j^T \psi(y_j) - B(\eta_j)\}$$

$$p(h_k) = \exp\{\lambda_k^T \varphi(h_k) - C(\lambda_k)\} \quad (29)$$

where $\phi(\cdot)$, $\psi(\cdot)$, and $\varphi(\cdot)$ are potentials over cliques formed by individual nodes, θ_i , η_j , and λ_k are the associated weights of potential functions, and $A(\cdot)$, $B(\cdot)$, and $C(\cdot)$ are log partition functions.

Through coupling the random variables in the log-domain and introducing other additional terms, we obtain the joint distribution $p(X, Y, H)$ as follows:

$$p(X, Y, H) \propto \exp\left\{ \sum_i \theta_i^T \phi(x_i) + \sum_j \eta_j^T \psi(y_j) + \sum_k \lambda_k^T \varphi(h_k) \right. \\ \left. + \sum_{ik} \phi(x_i)^T W_{ik} \varphi(h_k) + \sum_{jk} \psi(y_j)^T U_{jk} \varphi(h_k) \right\} \quad (30)$$

where $\phi(x_i)\varphi(h_k)$, $\psi(y_j)\varphi(h_k)$ are potentials over cliques consisting of pairwise linked nodes, and W_{ik} , U_{jk} are the associated weights of potential functions. From the joint distribution, we can derive the conditional distributions

$$p(x_i|H) \propto \exp\{\tilde{\theta}_i^T \phi(x_i) - A(\tilde{\theta}_i)\}$$

$$p(y_j|H) \propto \exp\{\tilde{\eta}_j^T \psi(y_j) - B(\tilde{\eta}_j)\}$$

$$p(h_k|X, Y) \propto \exp\{\tilde{\lambda}_k^T \varphi(h_k) - C(\tilde{\lambda}_k)\} \quad (31)$$

where the shifted parameters $\tilde{\theta}_i = \theta_i + \sum_k W_{ik} \varphi(h_k)$, $\tilde{\eta}_j = \eta_j + \sum_k U_{jk} \varphi(h_k)$, and $\tilde{\lambda}_k = \lambda_k + \sum_i W_{ik} \phi(x_i) + \sum_j U_{jk} \psi(y_j)$.

In training probabilistic models parameters are typically updated in order to maximize the *likelihood of the training data*. The updating rules can be obtained by taking derivative of the log-likelihood of the sample defined in Eq.(30) with respect to the model parameters. The multi-wing model can be directly obtained by extending the dual-wing model when the multi-modal input data are observed.

Further, Chen et al. [16] present a multi-view latent space Markov network and its large-margin extension that satisfies a

weak conditional independence assumption that data from different views and the response variables are conditionally independent given a set of latent variables. In addition, Xie and Xing [127] propose a multi-modal distance metric learning (MMDML) framework based on the multi-wing harmonium model and metric learning method by [128]. This MMDML provides a principled way to embed data of arbitrary modalities into a single latent space where distance supervision is leveraged.

4.2 Directly Learning A Parametric Embedding from Multi-View Input to Representation

From the framework of multi-view probabilistic models discussed in the previous section, we can see that the learned representation is usually associated with shared latent variables, specifically with their posterior distribution given the multi-view observed input. Further, this posterior distribution often becomes complicated and intractable if the designed models have hierarchical structures. It has to resort to sampling or approximate inference techniques, which need to endure the associated computational and approximation error cost. In addition, a posterior distribution over shared latent variables is not yet a reasonable feature vector that can be directly fed to the classifier. Therefore, if we intend to obtain stable deterministic feature values, an alternative non-probabilistic multi-view embedding learning paradigm is the directly parameterized feature or representation functions. The common perspective between these methods is that they learn a direct encoding for multi-view input. Consequently, in this section we review the related work from this perspective.

4.2.1 Partial Least Squares

Partial Least Squares (PLS) [129–131] is a wide class of methods for modeling relations between sets of observed variables. It has been a popular tool for regression and classification as well as dimensionality reduction, especially in the field of chemometrics [132, 133]. The underlying assumption of all PLS methods is that the observed data are generated by a process which is driven by a small number of latent variables. In particular, PLS creates orthogonal latent vectors by maximizing the covariance between different sets of variables.

Given a pair of datasets $X = [x_1, \dots, x_n] \in \mathbb{R}^{d_x \times n}$ and $Y = [y_1, \dots, y_n] \in \mathbb{R}^{d_y \times n}$, a k -dimensional PLS solution can be parameterized by a pair of matrices $W_x \in \mathbb{R}^{d_x \times k}$ and $W_y \in \mathbb{R}^{d_y \times k}$ [61]. The PLS problem can now be expressed as:

$$\begin{aligned} & \max_{W_x, W_y} \text{tr} (W_x^\top C_{xy} W_y) \\ & \text{s.t. } W_x^\top W_x = I, W_y^\top W_y = I. \end{aligned} \quad (32)$$

It can be shown that the columns of the optimal W_x and W_y correspond to the singular vectors of covariance matrix $C_{xy} = \mathbb{E}[xy^\top]$. Like the CCA objective, PLS is also an optimization of an expectation subject to fixed constraints.

In essence, CCA finds the directions of maximum correlation while PLS finds the directions of maximum covariance. Covariance and correlation are two different statistical measures for describing how variables covary. It has been shown that there are close connections between PLS and CCA in several aspects [130, 133]. Guo and Mu [134] investigate the CCA based methods, including linear CCA, regularized CCA, and kernel CCA, and compare them with the PLS models in solving the joint estimation

problem. In particular, they provide a consistent ranking of the above methods in estimating age, gender, and ethnicity.

Further, Li et al. [31] introduce a least square form of PLS, called cross-modal factor analysis (CFA). CFA aims to find orthogonal transformation matrices W_x and W_y by minimizing the following expression:

$$\begin{aligned} & \|X^\top W_x - Y^\top W_y\|_F^2 \\ & \text{subject to: } W_x^\top W_x = I, \quad W_y^\top W_y = I \end{aligned} \quad (33)$$

where $\|\cdot\|_F$ denotes the Frobenius norm. It can be easily verified that the above optimization problem in Eq.(33) has the same solution as that of PLS. Several extensions of CFA are presented by incorporating non-linearity and supervised information [135–137].

4.2.2 Cross-Modal Ranking

Motivated by incorporating ranking information into multi-modal embedding learning, cross-modal ranking has attracted much attention in the literature [138–140]. Bai et al. [138] present a supervised semantic indexing (SSI) model which defines a class of non-linear models that are discriminatively trained to map multi-modal input pairs into ranking scores.

In particular, SSI attempts to learn a similarity function $f(q, d)$ between a text query q and an image d according to a pre-defined ranking loss. The learned function f directly maps each text-image pair to a ranking score based on their semantic relevance. Given a text query $q \in \mathbb{R}^m$ and an image $d \in \mathbb{R}^n$, SSI intends to find a linear scoring function to measure the relevance of d given q :

$$f(q, d) = q^\top W d = \sum_{i=1}^m \sum_{j=1}^n q_i W_{ij} d_j \quad (34)$$

where $f(q, d)$ is defined as the score between the query q and the image d , and the parameter $W \in \mathbb{R}^{m \times n}$ captures the correspondence between the two different modalities of the data: W_{ij} represents the correlation between the i -th dimension of the text space and the j -th dimension of the image space. Note that this way of embedding allows both positive and negative correlations between different modalities since both positive and negative values are allowed in W_{ij} .

Given the similarity function in Eq.(34) and a set of tuples, where each tuple contains a query q , a relevant image d^+ and an irrelevant image d^- , SSI attempts to choose the scoring function $f(q, d)$ such that $f(q, d^+) > f(q, d^-)$, expressing that d^+ should be ranked higher than d^- . For this purpose, SSI exploits the margin ranking loss [141] which has already been widely used in information retrieval, and minimizes:

$$\sum_{(q, d^+, d^-)} \max(0, 1 - q^\top W d^+ + q^\top W d^-) \quad (35)$$

This optimization problem can be solved through stochastic gradient descent [142],

$$\begin{aligned} W \leftarrow & W + \lambda \left(q(d^+)^\top - q(d^-)^\top \right), \\ & \text{if } 1 - q^\top W d^+ + q^\top W d^- > 0 \end{aligned} \quad (36)$$

In fact, this method is a special margin ranking perceptron [143], which has been shown to be equivalent to SVM [144]. In contrast to classical SVM, stochastic training is highly scalable and is easy to implement for millions of training examples.

However, dealing with the models on all the pairs of multi-modalities input features is still computationally challenging. Thus, SSI also proposes several improvements to the above basic model for addressing this issue, including low-rank representation, sparsification, and correlated feature hashing. For more detailed information, please refer to [138].

Further, to exploit the advantage of online learning of kernel-based classifiers, Grangier and Bengio [140] propose a discriminative cross-modal ranking model called Passive-Aggressive Model for Image Retrieval (PAMIR), which not only adopts a learning criterion related to the final retrieval performance, but also considers different image kernels.

4.2.3 Cross-Modal Hashing

CCA and its extensions haven been widely applied to conduct cross-view similarity search [32, 52, 85]. A promising way to speed up the cross-view similarity search is the hashing technique which makes a tradeoff between accuracy and efficiency. Hence, several multi-modal hashing methods have been proposed for fast similarity search in multi-modal data [145–154]. The principle of the multi-modal hashing methods is to map the high dimensional multi-modal data into a common hash code so that similar cross-modal data objects have the same or similar hash codes.

Bronstein et al. [145] propose a hashing-based model, called cross-modal similarity sensitive hashing (CMSSH), which approaches the cross-modality similarity learning problem by embedding the multi-modal data into a common metric space. The similarity is parameterized by the embedding itself. The goal of cross-modality similarity learning is to construct the similarity function between points from different spaces, $X \in \mathbb{R}^{d_1}$ and $Y \in \mathbb{R}^{d_2}$. Assume that the unknown binary similarity function is $s : X \times Y \rightarrow \{\pm 1\}$; the classical cross-modality similarity learning aims at finding a binary similarity function \hat{s} on $X \times Y$ approximating s . Recent work attempts to solve the problem of cross-modality similarity leaning as an multi-view representation learning problem.

In particular, CMSSH proposes to construct two maps: $\xi : X \rightarrow \mathbb{H}^n$ and $\eta : Y \rightarrow \mathbb{H}^n$, where \mathbb{H}^n denotes the n -dimensional Hamming space. Such mappings encode the multi-modal data into two n -bit binary strings so that $d_{\mathbb{H}^n}(\xi(x), \eta(y))$ is small for $s(x, y) = +1$ and large for $s(x, y) = -1$ with a high probability. Consequently, this hamming embedding can be interpreted as cross-modal similarity-sensitive hashing, under which positive pairs have a high collision probability, while negative pairs are unlikely to collide. Such hashing also acts as a way of multi-modal dimensionality reduction when $d_1, d_2 \gg n$.

The n -dimensional Hamming embedding for X can be thought of as a vector $\xi(x) = (\xi_1(x), \dots, \xi_n(x))$ of binary embeddings of the form

$$\xi_i(x) = \begin{cases} 0 & \text{if } f_i(x) \leq 0, \\ 1 & \text{if } f_i(x) > 0, \end{cases} \quad (37)$$

parameterized by a projection $f_i : X \rightarrow \mathbb{R}$. Similarly, η_i is a binary mapping parameterized by projection $g_i : Y \rightarrow \mathbb{R}$.

Following the greedy approach [155], the Hamming metric can be constructed sequentially as a superposition of weak binary classifiers on pairs of data points,

$$h_i(x, y) = \begin{cases} +1 & \text{if } \xi_i(x) = \eta_i(y), \\ -1 & \text{otherwise,} \end{cases} = (2\xi_i(x) - 1)(2\eta_i(y) - 1), \quad (38)$$

Here, a simple strategy for the mappings is affine projection, such as $f_i(x) = p_i^\top + a_i$ and $g_i(y) = q_i^\top y + b_i$. It can be extended to complex projections easily.

Observing the resemblance to sequentially binary classifiers, boosted cross-modality similarity learning algorithms are introduced based on the standard AdaBoost procedure [156]. CMSSH has shown its utility and efficiency in several multi-view learning applications including cross-representation shape retrieval and alignment of multi-modal medical images.

However, CMSSH only considers the inter-view correlation but ignores the intra-view similarity [157]. Kumar and Udupa [146] extend Spectral Hashing [158] from the single view setting to the multi-view scenario and present cross view hashing (CVH), which attempts to find hash functions that map similar objects to similar codewords over all the views so that inter-view and intra-view similarities are both preserved. Gong and Lazebink [147] combine iterative quantization with CCA to exploit cross-modal embeddings for learning similarity preserving binary codes. Consequently, Zhen and Yang [148] present co-regularized hashing (CRH) for multi-modal data based on a boosted co-regularization framework. The hash functions for each bit of the hash codes are learned by solving DC (difference of convex functions) programs, while the learning for multiple bits is performed via a boosting procedure. Later Zhu et al. [149] introduce linear cross-modal hashing (LCMH), which adopts a “two-stage” strategy to learn cross-view hashing functions. The data within each modality are first encoded into a low-rank representation using the idea of anchor graph [159] and then hash functions for each modality are learned to map each modality’s low-rank space into a shared Hamming space. Song et al. [160] introduce an inter-media hashing (IMH) model by jointly capturing inter-media and intra-media consistency.

5 DEEP METHODS ON MULTI-VIEW REPRESENTATION LEARNING

Inspired by the success of deep neural networks [5, 6, 25], a variety of deep multi-view feature learning methods have been proposed to capture the high-level relationship between multi-view data. In this section, we continue to review the deep multi-view representation models from probabilistic and directly embedding perspectives based on consensus and complementarity principles.

5.1 Probabilistic Models

Restricted Boltzmann Machines (RBM) [161] is an undirected graphical model that can learn the distribution of training data. The model consists of stochastically visible units $\mathbf{v} \in \{0, 1\}^{d_v}$ and stochastically hidden units $\mathbf{h} \in \{0, 1\}^{d_h}$, which seeks to minimize the following energy function $E : \{0, 1\}^{d_v+d_h} \rightarrow \mathbb{R}$:

$$E(\mathbf{v}, \mathbf{h}; \theta) = - \sum_{i=1}^{d_v} \sum_{j=1}^{d_h} v_i W_{ij} h_j - \sum_{i=1}^{d_v} b_i v_i - \sum_{j=1}^{d_h} a_j h_j \quad (39)$$

where $\theta = \{\mathbf{a}, \mathbf{b}, \mathbf{W}\}$ are the model parameters. Consequently, the joint distribution over the visible and hidden units is defined by:

$$P(\mathbf{v}, \mathbf{h}; \theta) = \frac{1}{Z(\theta)} \exp(-E(\mathbf{v}, \mathbf{h}; \theta)). \quad (40)$$

When considering modeling visible real-valued or sparse count data, this RBM can be easily extended to corresponding variants, e.g., Gaussian RBM [125] and replicated softmax RBM [162].

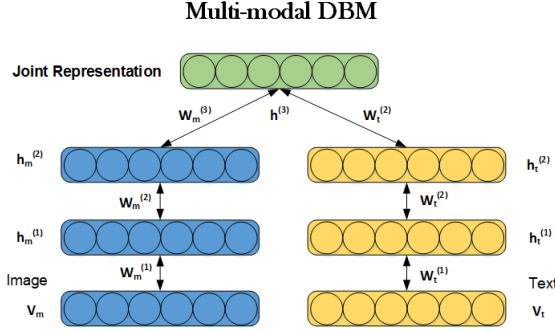


Fig. 5. The graphical model of deep multi-modal RBM (adapted from [17]), which models the joint distribution over image and text inputs.

A deep Boltzmann machine (DBM) is a generative network of stochastic binary units. It consists of a set of visible units $\mathbf{v} \in \{0, 1\}^{d_v}$, and a sequence of layers of hidden units $\mathbf{h}^{(1)} \in \{0, 1\}^{d_{h1}}, \mathbf{h}^{(2)} \in \{0, 1\}^{d_{h2}}, \dots, \mathbf{h}^{(L)} \in \{0, 1\}^{d_{hL}}$. Here only connections between hidden units are allowed in adjacent layers. Let us take a DBM with two hidden layers for example. By ignoring bias terms, the energy of the joint configuration $\{\mathbf{v}, \mathbf{h}\}$ is defined as

$$E(\mathbf{v}, \mathbf{h}; \theta) = -\mathbf{v}^\top W^{(1)} \mathbf{h}^{(1)} - \mathbf{h}^{(1)} W^{(2)} \mathbf{h}^{(2)} \quad (41)$$

where $\mathbf{h} = \{\mathbf{h}^{(1)}, \mathbf{h}^{(2)}\}$ represents the set of hidden units, and $\theta = \{W^{(1)}, W^{(2)}\}$ are the model parameters that denote visible-to-hidden and hidden-to-hidden symmetric interaction terms. Further, this binary-to-binary DBM can also be easily extended to modeling dense real-valued or sparse count data.

By extending the setup of the DBM, Srivastava and Salakhutdinov [17] propose a deep multi-modal RBM to model the relationship between imagery and text. In particular, each data modality is modeled using a separate two-layer DBM and then an additional layer of binary hidden units on top of them is added to learn the shared representation.

Let $\mathbf{v}_m \in \mathbb{R}^{d_{v_m}}$ denote an image input and $\mathbf{v}_t \in \mathbb{R}^{d_{v_t}}$ denote a text input. By ignoring bias terms on the hidden units for clarity, the distribution of \mathbf{v}_m in the image-specific two-layer DBM is given as follows:

$$\begin{aligned} P(\mathbf{v}_m; \theta) &= \sum_{\mathbf{h}^{(1)}, \mathbf{h}^{(2)}} P(\mathbf{v}_m, \mathbf{h}^{(1)}, \mathbf{h}^{(2)}; \theta) \\ &= \frac{1}{Z(\theta)} \sum_{\mathbf{h}^{(1)}, \mathbf{h}^{(2)}} \exp \left(-\sum_{i=1}^{d_{v_m}} \frac{(v_{mi} - b_i)^2}{2\sigma_i^2} + \sum_{i=1}^{d_{v_m}} \sum_{j=1}^{d_{h1}} \frac{v_{mi}}{\sigma_i} W_{ij}^{(1)} \right. \\ &\quad \left. + \sum_{j=1}^{d_{h1}} \sum_{l=1}^{d_{h2}} h_j^{(1)} W_{jl}^{(2)} h_l^{(2)} \right). \end{aligned} \quad (42)$$

Similarly, the text-specific two-layer DBM can also be defined by combining a replicated softmax model with a binary RBM.

Consequently, the deep multi-modal DBM has been presented by combining the image-specific and text-specific two-layer DBM with an additional layer of binary hidden units on top of them. The particular graphical model is shown in Figure 5. The joint

distribution over the multi-modal input can be written as:

$$P(\mathbf{v}^m, \mathbf{v}^t; \theta) = \sum_{\mathbf{h}_m^{(2)}, \mathbf{h}_t^{(2)}, \mathbf{h}^{(3)}} P(\mathbf{h}_m^{(2)}, \mathbf{h}_t^{(2)}, \mathbf{h}^{(3)}) \left(\sum_{\mathbf{h}_m^{(1)}} P(\mathbf{v}_m, \mathbf{h}_m^{(1)}, \mathbf{h}_m^{(2)}) \right) \left(\sum_{\mathbf{h}_t^{(1)}} P(\mathbf{v}_t, \mathbf{h}_t^{(1)}, \mathbf{h}_t^{(2)}) \right) \quad (43)$$

Like RBM, exact maximum likelihood learning in this model is also intractable, while efficient approximate learning can be implemented by using mean-field inference to estimate data-dependent expectations, and an MCMC based stochastic approximation procedure to approximate the model's expected sufficient statistics [6].

Multi-modal DBM has been widely used for multi-view representation learning [163–165]. Hu et al. [164] employ the multi-modal DBM to learn joint representation for predicting answers in cQA portal. Ge et al. [165] apply the multi-modal RBM to determining information trustworthiness, in which the learned joint representation denotes the consistent latent reasons that underline users' ratings from multiple sources. Pang and Ngo [166] propose to learn a joint density model for emotion prediction in user-generated videos with a deep multi-modal Boltzmann machine. This multi-modal DBM is exploited to model the joint distribution over visual, auditory, and textual features. Here Gaussian RBM is used to model the distributions over the visual and auditory features, and replicated softmax topic model is applied for mining the textual features.

Further, Sohn et al. [167] investigate an improved multi-modal RBM framework via minimizing the variation of information between data modalities through the shared latent representation. Recently, Ehrlich et al. [168] present a multi-task multi-modal RBM (MTM-RBM) approach for facial attribute classification. In particular, a multi-task RBM is proposed by extending the formulation of discriminative RBM [169] to account for multiple tasks. And then multi-task RBM is naturally extended to MTM-RBM by combining a collection of unimodal MT-RBM, one for each visible modality. Unlike the typical multi-modal RBM, the learned joint feature representation of MTM-RBM enables interaction between different tasks so that it is suited for multiple attribute classification.

5.2 Directly Deep Parametric Embedding from Multi-View Inputs to Representation

With the development of deep neural networks, many shallow multi-view embedding methods have been extended to deep ones, respectively. In this section, we review the deep multi-view feature learning methods from the directly parametric embedding perspective.

5.2.1 Multi-Modal Deep Autoencoders

Although Multi-modal RBMs achieve a great success in learning a shared representation, there are still limitations with them, e.g., there is no explicit objective for the models to discover correlations across the modalities such that some hidden units are tuned only for one modality while others are tuned only for the other. Multi-modal deep autoencoders [18, 170–172] gradually become good alternatives for learning a shared representation between modalities due to the sufficient flexibility of their objectives.

Inspired by denoising autoencoders [5], Ngiam et al. [18] propose to extract shared representations via training a bimodal

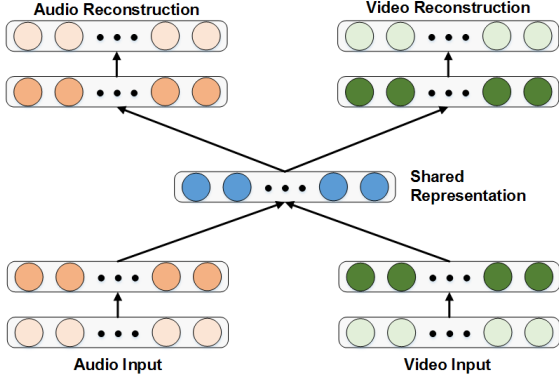


Fig. 6. The bimodal deep autoencoder (adapted from [18]).

deep autoencoder (Figure 6) using an augmented but noisy dataset with additional examples that have only a single modality as input. The key idea is to use greedy layer-wise training with an extension to RBMs with sparsity [173] followed by fine-tuning.

Further, Feng et al. [19] propose a correspondence autoencoder (Corr-AE) via constructing correlations between hidden representations of two uni-modal deep autoencoders. The details of the architecture of the basic Corr-AE is shown in Figure 7. As illustrated in Figure 7, this Corr-AE architecture consists of two subnetworks (each a basic deep autoencoder) that are connected by a predefined similarity measure on a specific coder layer. Each subnetwork in the Corr-AE serves for each modality.

Let $f(x; W_f)$ and $g(y; W_g)$ denote the mapping from the inputs $\{X, Y\}$ to the code layers, respectively. $\theta = \{W_f, W_g\}$ denotes the weight parameters in these two networks. Here the similarity measure between the i -th pair of image feature x_i and the given text feature y_i is defined as follows:

$$C(x_i, y_i; \theta) = \|f(x_i; W_f) - g(y_i; W_g)\|_2^2 \quad (44)$$

where f and g are logistic activation functions.

Consequently, the loss function on any pair of inputs is then defined as follows:

$$L(x_i, y_i; \theta) = (1 - \alpha) (L_I(x_i, y_i; \theta) + L_T(x_i, y_i; \theta)) + \alpha L_C(x_i, y_i; \theta) \quad (45)$$

where

$$\begin{aligned} L_I(x_i, y_i; \theta) &= \|x_i - \hat{x}_i\|_2^2 \\ L_T(x_i, y_i; \theta) &= \|y_i - \hat{y}_i\|_2^2 \\ L_C(x_i, y_i; \theta) &= C(x_i, y_i; \theta) \end{aligned}$$

L_I and L_T are the losses caused by data reconstruction errors for the given inputs of the two subnetworks, specifically image and text modality. L_C is the correlation loss and α is a parameter for trade-off between two groups of objectives. \hat{x}_i and \hat{y}_i are the reconstruction data from x_i and y_i respectively.

Overall, optimizing the objective in Eq.(45) enables Corr-AE to learn similar representations from bimodal features. Besides, based on two other multi-modal autoencoders [18], Corr-AE is extended to two other correspondence deep models, called Corr-Cross-AE and Corr-Full-AE.

Consequently, Silberer and Lapata [174] train stacked multi-modal autoencoder with semi-supervised objective to learn grounded meaning representations. Wang et al. [175] propose

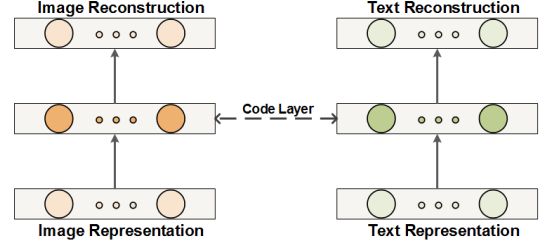


Fig. 7. The correspondence deep autoencoder (adapted from [19]).

an effective mapping mechanism based on stacked autoencoder for multi-modal retrieval. In particular, the cross-modal mapping functions are learned by optimizing an objective function which captures both intra-modal and inter-modal semantic relationships of data from heterogeneous sources.

Further, based on CCA and deep autoencoders, Wang et al. [20] propose deep canonically correlated autoencoders that also consist of two autoencoders and optimize the combination of canonical correlations between the learned bottleneck representations and the reconstruction errors of the autoencoders. Intuitively, this is the same principle as that of Corr-AE. The difference between them relies on the different similarity measures.

Recently, Rastegar et al. [176] suggest to exploit the cross weights between representations of modalities for gradually learning interactions of the modalities in a multi-modal deep autoencoder network. Theoretical analysis shows that considering these interactions in deep network manner (from low to high level) provides more intra-modality information. As opposed to the existing deep multi-modal autoencoders, this approach attempts to reconstruct the representation of each modality at a given level, with the representation of the other modalities in the previous layer.

5.2.2 Deep Cross-View Embedding Models

Deep cross-view embedding models have become increasingly popular in the applications including cross-media retrieval [177–180] and multi-modal distributional semantic learning [181, 182]. Frome et al. [177] propose a deep visual-semantic embedding model (DeViSE), which connects two deep neural networks by a cross-modal mapping. As shown in Figure 8, DeViSE is first initialized with a pre-trained neural network language model [183] and a pre-trained deep visual-semantic model [25]. Consequently, a linear transformation is exploited to map the representation at the top of the core visual model into the learned dense vector representations by the neural language model.

Following the setup of loss function in [138], DeViSE employs a combination of dot-product similarity and hinge rank loss so that the model has the ability of producing a higher dot-product similarity between the visual model output and the vector representation of the correct label than between the visual output and the other randomly chosen text terms. The per training example hinge rank loss is defined as follows:

$$\sum_{j \neq \text{label}} \max \left[0, \text{margin} - \vec{t}_{\text{label}}^T M \vec{v}(\text{image}) + \vec{t}_j^T M \vec{v}(\text{image}) \right] \quad (46)$$

where $\vec{v}(\text{image})$ is a column vector denoting the output of the top layer of the core visual network for the given image, M is the

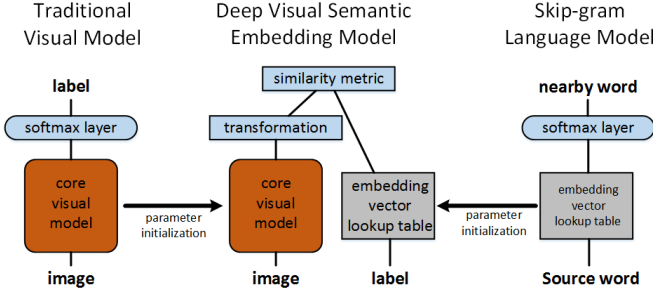


Fig. 8. The DeViSE model (adapted from [177]), which is initialized with parameters pre-trained at the lower layers of the visual object categorization network and the skip-gram language model.

mapping matrix of the linear transformation layer, \vec{t}_{label} is a row vector denoting the learned embedding vector for the provided text label, and \vec{t}_j are the embeddings of the other text terms. This DeViSE model is trained by asynchronous stochastic gradient descent on a distributed computing platform [184].

Inspired by the success of DeViSE, Norouzi et al. [185] propose a convex combination of semantic embedding model (ConSE) for mapping images into continuous semantic embedding spaces. Unlike DeViSE, this ConSE model keeps the softmax layer of the convolutional net intact. Given a test image, ConSE simply runs the convolutional classifier and considers the convex combination of the semantic embedding vectors from the top T predictions as its corresponding semantic embedding vector. Further, Fang et al. [186] develop a deep multi-modal similarity model that learns two neural networks to map image and text fragments to a common vector representation.

With the development of multi-modal distributional semantic models [187–190], deep cross-modal mapping is naturally exploited to learn the improved multimodal distributed semantic representation. Lazaridou et al. [182] introduce multimodal skip-gram models to extend the skip-gram model of [183] by taking visual information into account. In this extension, for a subset of the target words, relevant visual evidence from natural images is presented together with the corpus contexts. In particular, the model is designed to encourage the propagation of visual information to all words via a deep cross-modal ranking so that it can improve image labeling and retrieval in the zero-shot setup, where the test concepts are never seen during model training. Further, Dong et al. [180] present Word2VisualVec, a deep neural network architecture that learns to predict a deep visual encoding of textual input, and thus enables cross-media retrieval in a visual space.

In addition, Xu et al. [191] propose a unified framework that jointly models video and the corresponding text sentence. In this joint architecture, the goal is to learn a function $f(\mathcal{V}) : \mathcal{V} \rightarrow \mathcal{T}$, where \mathcal{V} represents the low-level features extracted from video, and \mathcal{T} is the high-level text description of the video. A joint model \mathcal{P} is designed to connect these two levels of information. It consists of three parts: compositional language model $M_L : T \rightarrow T_f$, deep video model $M_V : V \rightarrow V_f$, and a joint embedding model $E(V_f, T_f)$, such that

$$\mathcal{P} : M_V(V) \longrightarrow V_f \leftrightarrow E(V_f, T_f) \leftrightarrow T_f \longleftarrow M_L(T) \quad (47)$$

where V_f and T_f are the output of the deep video model and the compositional language model, respectively. In this joint

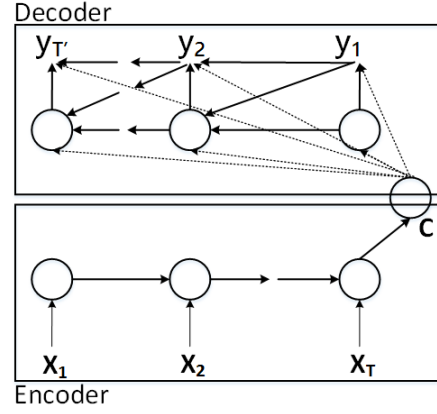


Fig. 9. The illustration of the RNN encoder-decoder (adapted from [194]).

embedding model, the distance between the outputs of the deep video model and those of the compositional language model in the joint space is minimized to make them alignment.

5.2.3 Multi-Modal Recurrent Neural Network

A recurrent neural network (RNN) [192] is a neural network which processes a variable-length sequence $\mathbf{x} = (x_1, \dots, x_T)$ through hidden state representation \mathbf{h} . At each time step t , the hidden state h_t of the RNN is estimated by

$$h_t = f(h_{t-1}, x_t) \quad (48)$$

where f is a non-linear activation function and is selected based on the requirement of data modeling. For example, a simple case may be a common element-wise logistic sigmoid function and a complex case may be a long short-term memory (LSTM) unit [193].

An RNN is known as its ability of learning a probability distribution over a sequence by being trained to predict the next symbol in a sequence. In this training, the prediction at each time step t is decided by the conditional distribution $p(x_t | x_{t-1}, \dots, x_1)$. For example, a multinomial distribution can be learned as output with a softmax activation function

$$p(x_{t,j} = 1 | x_{t-1}, \dots, x_1) = \frac{\exp(w_j h_t)}{\sum_{j'=1}^K \exp(w_{j'} h_t)} \quad (49)$$

where $j = 1, \dots, K$ denotes the possible symbol components and w_j are the corresponding rows of a weight matrix W . Further, based on the above probabilities, the probability of the sequence \mathbf{x} can be computed as

$$p(\mathbf{x}) = \prod_{t=1}^T p(x_t | x_{t-1}, \dots, x_1). \quad (50)$$

With this learned distribution, it is straightforward to generate a new sequence by iteratively generating a symbol at each time step.

Cho et al. [194] propose a RNN encoder-decoder model by exploiting RNN to connect multi-modal sequence. As shown in Figure 9, this neural network first encodes a variable-length source sequence into a fixed-length vector representation and then decodes this fixed-length vector representation back into a variable-length target sequence. In fact, it is a general method to learn the conditional distribution over an output sequence conditioned on

another input sequence, e.g., $p(y_1, \dots, y_{T'} | x_1, \dots, x_T)$, where the input and output sequence lengths T and T' can be different. In particular, the encoder of the proposed model is an RNN which sequentially encodes each symbol of an input sequence \mathbf{x} into the corresponding hidden state according to Eq.(48). After reading the end of the input sequence, a summary hidden state of the whole source sequence \mathbf{c} is acquired. The decoder of the proposed model is another RNN which is exploited to generate the target sequence by predicting the next symbol y_t with the hidden state h_t . Based on the recurrent property, both y_t and h_t are also conditioned on y_{t-1} and on the summary \mathbf{c} of the input sequence. Thus, the hidden state of the decoder at time t is computed by,

$$h_t = f(h_{t-1}, y_{t-1}, \mathbf{c}) \quad (51)$$

and the conditional distribution of the next symbol is

$$p(y_t | y_{t-1}, y_{t-2}, \dots, y_1, \mathbf{c}) = g(h_t, y_{t-1}, \mathbf{c}) \quad (52)$$

where g is an activation function and produces valid probabilities with a softmax. The main idea of the RNN-based encoder-decoder framework can be summarized by jointly training two RNNs to maximize the conditional log-likelihood

$$\max_{\theta} \frac{1}{N} \sum_{n=1}^N \log p_{\theta}(\mathbf{y}_n | \mathbf{x}_n) \quad (53)$$

where θ is the set of the model parameters and each pair $(\mathbf{x}_n, \mathbf{y}_n)$ consists of an input sequence and an output sequence from the training set. The model parameters can be estimated by a gradient-based algorithm.

Further, Sutskever et al. [195] also present a general end-to-end approach for multi-modal sequence to sequence learning based on deep LSTM networks, which are very useful for learning problems with long range temporal dependencies [193, 196]. The goal of this method is also to estimate the conditional probability $p(y_1, \dots, y_{T'} | x_1, \dots, x_T)$. Similar to [194], the conditional probability is computed by first obtaining the fixed dimensional representation v of the input sequence (x_1, \dots, x_T) with the encoding LSTM-based networks, and then computing the probability of $y_1, \dots, y_{T'}$ with the decoding LSTM-based networks whose initial hidden state is set to the representation v of x_1, \dots, x_T :

$$p(y_1, \dots, y_{T'} | x_1, \dots, x_T) = \prod_{t=1}^{T'} p(y_t | v, y_1, \dots, y_{t-1}) \quad (54)$$

where each $p(y_t | v, y_1, \dots, y_{t-1})$ distribution is represented with a softmax over all the words in the vocabulary.

Besides, multi-modal RNNs have been widely applied in image captioning [21, 22, 197], video captioning [23, 198, 199], visual question answering [200], and information retrieval [201]. Karpathy and Li [21] propose a multi-modal recurrent neural network architecture to generate new descriptions of image regions. Chen and Zitnick [202] explore the bi-directional mapping between images and their sentence-based descriptions with RNNs. Venugopalan et al. [199] introduce an end-to-end sequence model to generate captions for videos.

By applying attention mechanism [203] to visual recognition [204, 205], Xu et al. [35] introduce an attention based multi-modal RNN model, which trains the multi-modal RNN in a deterministic manner using the standard back-propagation. In particular, it incorporates a form of attention with two variants: a "hard" attention mechanism and a "soft" attention mechanism. The advantage of

the proposed model lies in attending to salient part of an image while generating its caption.

6 MULTI-VIEW REPRESENTATION LEARNING AS MANIFOLD ALIGNMENT

Another important perspective on multi-view representation learning is based on the manifold alignment. The key idea underlying this approach is to embed inputs from different domains to a new latent common space, simultaneously preserving topology of each input domain. Its premise is the manifold hypothesis, according to which high-dimensional real-world data are expected to concentrate in the vicinity of a low-dimensional manifold, embedded in high dimensional input space. In particular, this prior is well suited for datasets such as images, sounds and texts, as this information is not natural signals. Since most data sources can be modeled by manifolds, manifold alignment can be used to align the underlying structures across different data views. With this perspective, the multi-view representation learning task can be seen as finding the relationship among the structures of manifolds from the different views of data.

One of the pioneering efforts in manifold alignment with given coordinates is the semi-supervised alignment by Ham et al. [24]. Given certain labeled samples by the ordinal index l , semi-supervised alignment aims to find a mapping defined on the vertices of the graph $f : V \mapsto R$ that matches the known target values for the labeled vertices. This can be solved by directly finding $\arg \min_f |f_i - s_i|$ ($i \in l$) where s is the vector of target value. Since only a small number of labeled examples are provided, it is important to exploit manifold structure in the data when constructing the mapping function. In particular, graph Laplacian matrix L provides this structural information. The semi-supervised alignment problem can be solved by minimizing the following objective function:

$$C(f) = \sum_i \mu |f_i - s_i|^2 + f^T L f \quad (55)$$

where the first term is the loss function, and the second term enforces smoothness along the manifold. The optimum mapping function f is easily obtained by a linear transform.

This semi-supervised alignment is similar to manifold ranking [206], which learns to rank on data manifolds. They both take advantage of the manifold learning to do alignment between different types of data. To exploit the high level geometry structure embedded in the data samples, Mao et al. [207] extend the original semi-supervised alignment and propose a method called parallel field alignment retrieval (PFAR), which investigates alignment framework from the perspective of parallel vector fields.

In addition, Ham et al. [24] also introduce manifold alignment with pairwise correspondence, which builds connections between multiple data sets by aligning their underlying manifolds. In particular, multi-view input data sets $\{X, Y\}$ have subsets X_l and Y_l which are in pairwise alignment by the indices $x_i \leftrightarrow y_i$, ($i \in l$). Then we intend to determine how to match the remaining examples using aligned manifold embeddings. Considering that embedding coordinates for each data set should take similar values for corresponding pairs, the multi-view manifold embedding can be defined by generalizing the single graph embedding algorithm as follows:

$$C(f, g) = \mu \sum_{i \in l} |f_i - g_i| + f^T L^x f + g^T L^y g \quad (56)$$

where f and g denote real-valued functions defined on the respective graphs of X and Y ; L^x and L^y are the graph Laplacian matrices of X and Y . The first term penalizes the difference between f and g on the corresponding vertices, and the second and third terms impose smoothness constraints on f and g based on the respective graphs.

This graph algorithm is able to robustly align the underlying manifold structure across multi-view data sets. Even with a small number of paired samples provided, the algorithm is capable of estimating a common low-dimensional embedding space which can be used in cross-view retrieval task. The main concern about this algorithm is the computational cost, which lies in finding the spectral decomposition of a large matrix. Methods for calculating eigenvectors of large sparse matrices can be employed to speed up the computation of the embeddings.

7 CONCLUSION

Multi-view representation learning has attracted much attention in machine learning and data mining areas. This paper introduces several important principles for multi-view representation learning: correlation, consensus, and complementarity principles. Consequently, we first review the representative methods and theories of multi-view representation learning based on correlation principle, especially on canonical correlation analysis (CCA) and its extensions. And then from the viewpoint of consensus and complementarity principles we investigate the advances of multi-view representation learning that ranges from shallow methods including multi-modal topic learning, multi-view sparse coding, and multi-view latent space Markov networks, to deep methods including multi-modal restricted Boltzmann machines, multi-modal autoencoders, and multi-modal recurrent neural networks. Further, we also provide an important perspective for multi-view representation learning from manifold alignment. This survey aims to provide an insightful picture of the theoretical basis and the current development in the field of multi-view representation learning and to help find the most appropriate methodologies for particular applications.

REFERENCES

- [1] H. Hotelling, “Relations between two sets of variates,” *Biometrika*, vol. 28, no. 3/4, pp. 321–377, 1936.
- [2] F. R. Bach and M. I. Jordan, “Kernel independent component analysis,” *Journal of Machine Learning Research*, vol. 3, pp. 1–48, 2002.
- [3] D. R. Hardoon, S. R. Szedmak, and J. R. Shawe-taylor, “Canonical correlation analysis: An overview with application to learning methods,” *Neural Comput.*, vol. 16, no. 12, pp. 2639–2664, Dec. 2004.
- [4] S. Sun, “A survey of multi-view machine learning,” *Neural Computing and Applications*, vol. 23, no. 7–8, pp. 2031–2038, 2013.
- [5] P. Vincent, H. Larochelle, Y. Bengio, and P.-A. Manzagol, “Extracting and composing robust features with denoising autoencoders,” in *ICML*, 2008, pp. 1096–1103.
- [6] R. Salakhutdinov and G. E. Hinton, “Deep boltzmann machines,” in *AISTATS*, vol. 1, 2009, p. 3.
- [7] Y. Bengio, A. Courville, and P. Vincent, “Representation learning: A review and new perspectives,” *IEEE transactions on pattern analysis and machine intelligence*, vol. 35, no. 8, pp. 1798–1828, 2013.
- [8] G. Andrew, R. Arora, J. A. Bilmes, and K. Livescu, “Deep canonical correlation analysis,” in *ICML*, 2013, pp. 1247–1255.
- [9] D. A. Cohn and T. Hofmann, “The missing link - A probabilistic model of document content and hypertext connectivity,” in *NIPS*, 2000, pp. 430–436.
- [10] K. Barnard, P. Duygulu, D. Forsyth, N. de Freitas, D. M. Blei, and M. I. Jordan, “Matching words and pictures,” *J. Mach. Learn. Res.*, vol. 3, pp. 1107–1135, Mar. 2003.
- [11] D. M. Blei and M. I. Jordan, “Modeling annotated data,” in *SIGIR*, 2003, pp. 127–134.
- [12] Y. Jia, M. Salzmann, and T. Darrell, “Factorized latent spaces with structured sparsity,” in *NIPS*, 2010, pp. 982–990.
- [13] T. Cao, V. Jojic, S. Modla, D. Powell, K. Czumek, and M. Niethammer, “Robust multimodal dictionary learning,” in *MICCAI*, 2013, pp. 259–266.
- [14] W. Liu, D. Tao, J. Cheng, and Y. Tang, “Multiview hessian discriminative sparse coding for image annotation,” *Computer Vision and Image Understanding*, vol. 118, pp. 50–60, 2014.
- [15] E. P. Xing, R. Yan, and A. G. Hauptmann, “Mining associated text and images with dual-wing harmoniums,” in *UAI*, 2005, pp. 633–641.
- [16] N. Chen, J. Zhu, and E. P. Xing, “Predictive subspace learning for multi-view data: a large margin approach,” in *NIPS*, 2010, pp. 361–369.
- [17] N. Srivastava and R. Salakhutdinov, “Multimodal learning with deep boltzmann machines,” in *NIPS*, 2012, pp. 2231–2239.
- [18] J. Ngiam, A. Khosla, M. Kim, J. Nam, H. Lee, and A. Y. Ng, “Multimodal deep learning,” in *ICML*, 2011, pp. 689–696.
- [19] F. Feng, X. Wang, and R. Li, “Cross-modal retrieval with correspondence autoencoder,” in *ACM Multimedia*, 2014, pp. 7–16.
- [20] W. Wang, R. Arora, K. Livescu, and J. A. Bilmes, “On deep multi-view representation learning,” in *ICML*, 2015, pp. 1083–1092.
- [21] A. Karpathy and F. Li, “Deep visual-semantic alignments for generating image descriptions,” *CoRR*, vol. abs/1412.2306, 2014.
- [22] J. Mao, W. Xu, Y. Yang, J. Wang, Z. Huang, and A. Yuille, “Deep captioning with multimodal recurrent neural networks (m-rnn),” *arXiv preprint arXiv:1412.6632*, 2014.
- [23] J. Donahue, L. Anne Hendricks, S. Guadarrama, M. Rohrbach, S. Venugopalan, K. Saenko, and T. Darrell, “Long-term recurrent convolutional networks for visual recognition and description,” in *CVPR*, 2015, pp. 2625–2634.
- [24] J. Ham, D. Lee, and L. Saul, “Semisupervised alignment of manifolds,” in *10th International Workshop on Artificial Intelligence and Statistics*, 2005, pp. 120–127.
- [25] A. Krizhevsky, I. Sutskever, and G. E. Hinton, “Imagenet classification with deep convolutional neural networks,” in *NIPS*, 2012, pp. 1097–1105.
- [26] J. Bleiholder and F. Naumann, “Data fusion,” *ACM Comput. Surv.*, vol. 41, no. 1, Jan. 2009.
- [27] P. K. Atrey, M. A. Hossain, A. El-Saddik, and M. S. Kankanhalli, “Multimodal fusion for multimedia analysis: a survey,” *Multimedia Syst.*, vol. 16, no. 6, pp. 345–379, 2010.
- [28] C. Xu, D. Tao, and C. Xu, “A survey on multi-view learning,” *arXiv preprint arXiv:1304.5634*, 2013.
- [29] D. Lahat, T. Adali, and C. Jutten, “Multimodal data fusion: An overview of methods, challenges, and prospects,” *Proceedings of the IEEE*, vol. 103, no. 9, pp. 1449–1477, 2015.
- [30] A. Wiesel, M. Kliger, and A. O. Hero, III, “A greedy approach to sparse canonical correlation analysis,” *ArXiv e-prints*, 2008.
- [31] D. Li, N. Dimitrova, M. Li, and I. K. Sethi, “Multimedia content processing through cross-modal association,” in *ACM Multimedia*, 2003, pp. 604–611.
- [32] N. Rasiwasia, J. Costa Pereira, E. Coviello, G. Doyle, G. R. Lanckriet, R. Levy, and N. Vasconcelos, “A new approach to cross-modal multimedia retrieval,” in *ACM Multimedia*, 2010, pp. 251–260.
- [33] D. Kiela and L. Bottou, “Learning image embeddings using convolutional neural networks for improved multi-modal semantics,” in *EMNLP*, 2014, pp. 36–45.

[34] G. Collell, T. Zhang, and M. Moens, “Imagined visual representations as multimodal embeddings,” in *AAAI*, 2017, pp. 4378–4384.

[35] K. Xu, J. Ba, R. Kiros, K. Cho, A. C. Courville, R. Salakhutdinov, R. S. Zemel, and Y. Bengio, “Show, attend and tell: Neural image caption generation with visual attention,” *CoRR*, vol. abs/1502.03044, 2015.

[36] A. P. Singh and G. J. Gordon, “Relational learning via collective matrix factorization,” in *SIGKDD*, 2008, pp. 650–658.

[37] B. Long, Z. M. Zhang, and P. S. Yu, “A probabilistic framework for relational clustering,” in *KDD*, 2007, pp. 470–479.

[38] S. Gunasekar, M. Yamada, D. Yin, and Y. Chang, “Consistent collective matrix completion under joint low rank structure,” in *AISTATS*, 2015.

[39] C. Lan, X. Li, Y. Deng, and J. Huan, “Partial collective matrix factorization and its pac bound,” 2016.

[40] E. Kidron, Y. Y. Schechner, and M. Elad, “Pixels that sound,” in *CVPR (1)*. IEEE Computer Society, 2005, pp. 88–95.

[41] L. Sun, S. Ji, and J. Ye, “A least squares formulation for canonical correlation analysis,” in *ICML*, 2008, pp. 1024–1031.

[42] D. P. Foster, R. Johnson, and T. Zhang, “Multi-view dimensionality reduction via canonical correlation analysis,” Tech. Rep., 2008.

[43] L. Sun, B. Ceran, and J. Ye, “A scalable two-stage approach for a class of dimensionality reduction techniques,” in *KDD*, 2010, pp. 313–322.

[44] H. Avron, C. Boutsidis, S. Toledo, and A. Zouzias, “Efficient dimensionality reduction for canonical correlation analysis,” in *ICML*, 2013, pp. 347–355.

[45] X. Z. Fern, C. E. Brodley, and M. A. Friedl, “Correlation clustering for learning mixtures of canonical correlation models,” in *SDM*, 2005, pp. 439–448.

[46] M. B. Blaschko and C. H. Lampert, “Correlational spectral clustering,” in *CVPR*, 2008.

[47] K. Chaudhuri, S. M. Kakade, K. Livescu, and K. Sridharan, “Multi-view clustering via canonical correlation analysis,” in *ICML*, 2009, pp. 129–136.

[48] S. M. Kakade and D. P. Foster, “Multi-view regression via canonical correlation analysis,” in *COLT*, 2007, pp. 82–96.

[49] B. McWilliams, D. Balduzzi, and J. M. Buhmann, “Correlated random features for fast semi-supervised learning,” in *NIPS*, 2013, pp. 440–448.

[50] P. S. Dhillon, D. P. Foster, and L. H. Ungar, “Multi-view learning of word embeddings via CCA,” in *NIPS*, 2011, pp. 199–207.

[51] P. S. Dhillon, J. Rodu, D. P. Foster, and L. H. Ungar, “Using CCA to improve CCA: A new spectral method for estimating vector models of words,” in *ICML*, 2012.

[52] Y. Gong, Q. Ke, M. Isard, and S. Lazebnik, “A multi-view embedding space for modeling internet images, tags, and their semantics,” *International Journal of Computer Vision*, vol. 106, no. 2, pp. 210–233, 2014.

[53] T. Kim, J. Kittler, and R. Cipolla, “Discriminative learning and recognition of image set classes using canonical correlations,” *IEEE Trans. Pattern Anal. Mach. Intell.*, vol. 29, no. 6, pp. 1005–1018, 2007.

[54] Y. Zhang and J. G. Schneider, “Multi-label output codes using canonical correlation analysis,” in *AISTATS*, 2011, pp. 873–882.

[55] Y. Su, Y. Fu, X. Gao, and Q. Tian, “Discriminant learning through multiple principal angles for visual recognition,” *IEEE Trans. Image Processing*, vol. 21, no. 3, pp. 1381–1390, 2012.

[56] G. H. Golub and H. Zha, “The canonical correlations of matrix pairs and their numerical computation,” Stanford, CA, USA, Tech. Rep., 1992.

[57] J. R. Kettenring, “Canonical analysis of several sets of variables,” *Biometrika*, vol. 58, no. 3, pp. 433–451, 1971.

[58] H. Avron, C. Boutsidis, S. Toledo, and A. Zouzias, “Efficient dimensionality reduction for canonical correlation analysis,” *SIAM J. Scientific Computing*, vol. 36, no. 5, 2014.

[59] J. A. Tropp, “Improved analysis of the subsampled randomized hadamard transform,” *CoRR*, vol. abs/1011.1595, 2010.

[60] Y. Lu and D. P. Foster, “large scale canonical correlation analysis with iterative least squares,” in *NIPS*, 2014, pp. 91–99.

[61] R. Arora, A. Cotter, K. Livescu, and N. Srebro, “Stochastic optimization for PCA and PLS,” in *50th Annual Allerton Conference on Communication, Control, and Computing, Allerton 2012, Allerton Park & Retreat Center, Monticello, IL, USA, October 1-5, 2012*, 2012, pp. 861–868.

[62] Z. Ma, Y. Lu, and D. P. Foster, “Finding linear structure in large datasets with scalable canonical correlation analysis,” in *ICML*, 2015, pp. 169–178.

[63] W. Wang, J. Wang, and N. Srebro, “Globally convergent stochastic optimization for canonical correlation analysis,” *CoRR*, vol. abs/1604.01870, 2016.

[64] R. Ge, C. Jin, S. M. Kakade, P. Netrapalli, and A. Sidford, “Efficient algorithms for large-scale generalized eigenvector computation and canonical correlation analysis,” *CoRR*, vol. abs/1604.03930, 2016.

[65] F. R. Bach and M. I. Jordan, “A probabilistic interpretation of canonical correlation analysis,” Department of Statistics, University of California, Berkeley, Tech. Rep., 2005.

[66] M. W. Browne, “The maximum-likelihood solution in inter-battery factor analysis,” *British Journal of Mathematical and Statistical Psychology*, vol. 32, no. 1, pp. 75–86, 1979.

[67] C. Archambeau, N. Delannay, and M. Verleysen, “Robust probabilistic projections,” in *ICML*, 2006, pp. 33–40.

[68] C. Fyfe and G. Leen, “Stochastic processes for canonical correlation analysis,” in *ESANN*, 2006, pp. 245–250.

[69] A. Klami and S. Kaski, “Local dependent components,” in *ICML*, 2007, pp. 425–432.

[70] C. Wang, “Variational bayesian approach to canonical correlation analysis,” *IEEE Trans. Neural Networks*, vol. 18, no. 3, pp. 905–910, 2007.

[71] I. Huopaniemi, T. Suvitaval, J. Nikkilä, M. Oresic, and S. Kaski, “Two-way analysis of high-dimensional collinear data,” *Data Min. Knowl. Discov.*, vol. 19, no. 2, pp. 261–276, 2009.

[72] R. Tibshirani, “Regression shrinkage and selection via the lasso,” *Journal of the Royal Statistical Society (Series B)*, vol. 58, pp. 267–288, 1996.

[73] D. R. Hardoon and J. Shawe-Taylor, “Sparse canonical correlation analysis,” Department of Computer Science, University College London, Tech. Rep., 2007.

[74] S. Waaijenborg, P. C. Verselelew de Witt Hamer, and A. H. Zwinderman, “Quantifying the association between gene expressions and DNA-markers by penalized canonical correlation analysis,” *Statistical applications in genetics and molecular biology*, vol. 7, no. 1, 2008.

[75] B. Efron, T. Hastie, I. Johnstone, and R. Tibshirani, “Least angle regression,” *Annals of Statistics*, vol. 32, pp. 407–499, 2004.

[76] M. Belkin, P. Niyogi, and V. Sindhwani, “Manifold regularization: A geometric framework for learning from labeled and unlabeled examples,” *J. Mach. Learn. Res.*, vol. 7, pp. 2399–2434, Dec. 2006.

[77] A. d’Aspremont, L. E. Ghaoui, M. I. Jordan, and G. R. G. Lanckriet, “A direct formulation for sparse PCA using semidefinite programming,” *SIAM Review*, vol. 49, no. 3, pp. 434–448, 2007.

[78] D. Torres, D. Turnbull, L. Barrington, B. Sriperumbudur, and G. Lanckriet, “Finding musically meaningful words by sparse cca,” *NIPS WMBC ’07*, December 2007.

[79] A. d’Aspremont, F. R. Bach, and L. E. Ghaoui, “Full regularization path for sparse principal component analysis,” in *ICML*, 2007, pp. 177–184.

[80] D. M. Witten, T. Hastie, and R. Tibshirani, “A penalized matrix decomposition, with applications to sparse principal components and canonical correlation analysis,” *Biostatistics*,

2009.

[81] X. Chen, H. Liu, and J. G. Carbonell, "Structured sparse canonical correlation analysis," in *AISTATS*, 2012, pp. 199–207.

[82] P. L. Lai and C. Fyfe, "Kernel and nonlinear canonical correlation analysis," in *IJCNN* (4), 2000, p. 614.

[83] S. Akaho, "A kernel method for canonical correlation analysis," in *International Meeting of the Psychometric Society*, 2001.

[84] R. Socher and F. Li, "Connecting modalities: Semi-supervised segmentation and annotation of images using unaligned text corpora," in *CVPR*, 2010, pp. 966–973.

[85] S. J. Hwang and K. Grauman, "Learning the relative importance of objects from tagged images for retrieval and cross-modal search," *International Journal of Computer Vision*, vol. 100, no. 2, pp. 134–153, 2012.

[86] Y. Yamanishi, J. Vert, A. Nakaya, and M. Kanehisa, "Extraction of correlated gene clusters from multiple genomic data by generalized kernel canonical correlation analysis," in *ICISMB*, 2003, pp. 323–330.

[87] M. B. Blaschko, J. A. Shelton, A. Bartels, C. H. Lampert, and A. Gretton, "Semi-supervised kernel canonical correlation analysis with application to human fmri," *Pattern Recognition Letters*, vol. 32, no. 11, pp. 1572–1583, 2011.

[88] A. Trivedi, P. Rai, S. L. DuVall, and H. Daumé, III, "Exploiting tag and word correlations for improved webpage clustering," in *Proceedings of the 2Nd International Workshop on Search and Mining User-generated Contents*, ser. SMUC '10, 2010, pp. 3–12.

[89] R. Arora and K. Livescu, "Kernel CCA for multi-view learning of acoustic features using articulatory measurements," in *MLSLP*, 2012, pp. 34–37.

[90] —, "Multi-view cca-based acoustic features for phonetic recognition across speakers and domains," in *ICASSP*, 2013, pp. 7135–7139.

[91] A. Gretton, R. Herbrich, A. J. Smola, O. Bousquet, and B. Schölkopf, "Kernel methods for measuring independence," *Journal of Machine Learning Research*, vol. 6, pp. 2075–2129, 2005.

[92] B. Schölkopf and A. J. Smola, *Learning with Kernels: Support Vector Machines, Regularization, Optimization, and Beyond*. The MIT Press, 2001.

[93] M. Kuss and T. Graepel, "The geometry of kernel canonical correlation analysis," Max Planck Institute for Biological Cybernetics, Tübingen, Germany, Tech. Rep. 108, may 2003.

[94] K. Fukumizu, F. R. Bach, and A. Gretton, "Statistical consistency of kernel canonical correlation analysis," *Journal of Machine Learning Research*, vol. 8, pp. 361–383, 2007.

[95] D. R. Hardoon and J. Shawe-Taylor, "Convergence analysis of kernel canonical correlation analysis: theory and practice," *Machine Learning*, vol. 74, no. 1, pp. 23–38, 2009.

[96] J. Cai and H. Sun, "Convergence rate of kernel canonical correlation analysis," *Science China Mathematics*, vol. 54, no. 10, pp. 2161–2170, 2011.

[97] M. Brand, "Incremental singular value decomposition of uncertain data with missing values," in *ECCV*, 2002, pp. 707–720.

[98] C. K. I. Williams and M. W. Seeger, "Using the nyström method to speed up kernel machines," in *NIPS*, 2000, pp. 682–688.

[99] T. Yang, Y. Li, M. Mahdavi, R. Jin, and Z. Zhou, "Nyström method vs random fourier features: A theoretical and empirical comparison," in *NIPS*, 2012, pp. 485–493.

[100] Q. V. Le, T. Sarlós, and A. J. Smola, "Fastfood - computing hilbert space expansions in loglinear time," in *ICML*, 2013, pp. 244–252.

[101] D. Lopez-Paz, S. Sra, A. J. Smola, Z. Ghahramani, and B. Schölkopf, "Randomized nonlinear component analysis," in *ICML*, 2014, pp. 1359–1367.

[102] W. Wang and K. Livescu, "Large-scale approximate kernel canonical correlation analysis," *CoRR*, vol. abs/1511.04773, 2015.

[103] S. Becker and G. E. Hinton, "Self-organizing neural network that discovers surfaces in random-dot stereograms," *Nature*, vol. 355, no. 6356, pp. 161–163, 1992.

[104] S. Becker, "Mutual information maximization: Models of cortical self-organization," *Network : Computation in Neural Systems*, vol. 7, pp. 7–31, 1996.

[105] P. L. Lai and C. Fyfe, "Canonical correlation analysis using artificial neural networks," in *ESANN*, 1998, pp. 363–368.

[106] —, "A neural implementation of canonical correlation analysis," *Neural Networks*, vol. 12, no. 10, pp. 1391–1397, 1999.

[107] W. W. Hsieh, "Nonlinear canonical correlation analysis by neural networks," *Neural Networks*, vol. 13, no. 10, pp. 1095–1105, 2000.

[108] W. Wang, R. Arora, K. Livescu, and J. A. Bilmes, "Unsupervised learning of acoustic features via deep canonical correlation analysis," in *ICASSP*, 2015, pp. 4590–4594.

[109] A. Lu, W. Wang, M. Bansal, K. Gimpel, and K. Livescu, "Deep multilingual correlation for improved word embeddings," in *HLT-NAACL*, 2015, pp. 250–256.

[110] W. Wang, R. Arora, K. Livescu, and N. Srebro, "Stochastic optimization for deep CCA via nonlinear orthogonal iterations," in *Allerton*, 2015, pp. 688–695.

[111] F. Yan and K. Mikolajczyk, "Deep correlation for matching images and text," in *CVPR*, 2015, pp. 3441–3450.

[112] D. M. Blei, A. Y. Ng, and M. I. Jordan, "Latent dirichlet allocation," *Journal of Machine Learning Research*, vol. 3, pp. 993–1022, 2003.

[113] J. Zhu, L. Li, F. Li, and E. P. Xing, "Large margin learning of upstream scene understanding models," in *NIPS*, 2010, pp. 2586–2594.

[114] C. Wang, D. M. Blei, and F. Li, "Simultaneous image classification and annotation," in *CVPR*, 2009, pp. 1903–1910.

[115] D. M. Blei and J. D. McAuliffe, "Supervised topic models," in *NIPS*, 2007, pp. 121–128.

[116] L. Li and F. Li, "What, where and who? classifying events by scene and object recognition," in *ICCV*, 2007, pp. 1–8.

[117] L. Cao and F. Li, "Spatially coherent latent topic model for concurrent segmentation and classification of objects and scenes," in *ICCV*, 2007, pp. 1–8.

[118] L. Li, R. Socher, and F. Li, "Towards total scene understanding: Classification, annotation and segmentation in an automatic framework," in *CVPR*, 2009, pp. 2036–2043.

[119] C. Nguyen, D. Zhan, and Z. Zhou, "Multi-modal image annotation with multi-instance multi-label LDA," in *IJCAI*, 2013.

[120] C. M. Bishop, *Pattern recognition and machine learning*. Springer, 2006.

[121] Y. Han, F. Wu, D. Tao, J. Shao, Y. Zhuang, and J. Jiang, "Sparse unsupervised dimensionality reduction for multiple view data," *IEEE Trans. Circuits Syst. Video Techn.*, vol. 22, no. 10, pp. 1485–1496, 2012.

[122] J. Yu, Y. Rui, and D. Tao, "Click prediction for web image reranking using multimodal sparse coding," *IEEE Transactions on Image Processing*, vol. 23, no. 5, pp. 2019–2032, 2014.

[123] Y. Zhuang, Y. Wang, F. Wu, Y. Zhang, and W. Lu, "Supervised coupled dictionary learning with group structures for multi-modal retrieval," in *AAAI*, 2013.

[124] F. Wu, Z. Yu, Y. Yang, S. Tang, Y. Zhang, and Y. Zhuang, "Sparse multi-modal hashing," *IEEE Trans. Multimedia*, vol. 16, no. 2, pp. 427–439, 2014.

[125] M. Welling, M. Rosen-Zvi, and G. E. Hinton, "Exponential family harmoniums with an application to information retrieval," in *NIPS*, 2004, pp. 1481–1488.

[126] G. E. Hinton, "Training products of experts by minimizing contrastive divergence," *Neural Computation*, vol. 14, no. 8, pp. 1771–1800, 2002.

[127] P. Xie and E. P. Xing, "Multi-modal distance metric learning," in *IJCAI*, 2013, pp. 1806–1812.

[128] E. P. Xing, A. Y. Ng, M. I. Jordan, and S. J. Russell, "Distance metric learning with application to clustering with side-information," in *NIPS*, 2002, pp. 505–512.

- [129] H. Wold, "Soft modeling: the basic design and some extensions," *Systems under indirect observation*, vol. 2, pp. 589–591, 1982.
- [130] R. Rosipal and N. Krämer, *Overview and Recent Advances in Partial Least Squares*, 2006, pp. 34–51.
- [131] W. R. Schwartz, A. Kembhavi, D. Harwood, and L. S. Davis, "Human detection using partial least squares analysis," in *ICCV*, 2009, pp. 24–31.
- [132] S. Wold, M. Sjström, and L. Eriksson, "PLs-regression: a basic tool of chemometrics," *Chemometrics and Intelligent Laboratory Systems*, vol. 58, pp. 109–130, 2001.
- [133] M. Barker and W. Rayens, "Partial least squares for discrimination," *Journal of Chemometrics*, vol. 17, no. 3, pp. 166 – 173, 2003.
- [134] G. Guo and G. Mu, "Joint estimation of age, gender and ethnicity: CCA vs. PLS," in *FG*, 2013, pp. 1–6.
- [135] Y. Wang, L. Guan, and A. N. Venetsanopoulos, "Kernel cross-modal factor analysis for information fusion with application to bimodal emotion recognition," *IEEE Transactions on Multimedia*, vol. 14, no. 3-1, pp. 597–607, 2012.
- [136] J. C. Pereira, E. Coviello, G. Doyle, N. Rasiwasia, G. R. G. Lanckriet, R. Levy, and N. Vasconcelos, "On the role of correlation and abstraction in cross-modal multimedia retrieval," *IEEE Trans. Pattern Anal. Mach. Intell.*, vol. 36, no. 3, pp. 521–535, 2014.
- [137] J. Wang, H. Wang, Y. Tu, K. Duan, Z. Zhan, and S. Chekuri, "Supervised cross-modal factor analysis," *CoRR*, vol. abs/1502.05134, 2015.
- [138] B. Bai, J. Weston, D. Grangier, R. Collobert, K. Sadamasa, Y. Qi, O. Chapelle, and K. Q. Weinberger, "Learning to rank with (a lot of) word features," *Inf. Retr.*, vol. 13, no. 3, pp. 291–314, 2010.
- [139] J. Weston, S. Bengio, and N. Usunier, "Large scale image annotation: learning to rank with joint word-image embeddings," *Machine Learning*, vol. 81, no. 1, pp. 21–35, 2010.
- [140] D. Grangier and S. Bengio, "A discriminative kernel-based approach to rank images from text queries," *IEEE Trans. Pattern Anal. Mach. Intell.*, vol. 30, no. 8, pp. 1371–1384, 2008.
- [141] R. Herbrich, T. Graepel, and K. Obermayer, "Large margin rank boundaries for ordinal regression," in *Advances in Large Margin Classifiers*. Cambridge, MA: MIT Press, 2000.
- [142] C. J. C. Burges, T. Shaked, E. Renshaw, A. Lazier, M. Deeds, N. Hamilton, and G. N. Hullender, "Learning to rank using gradient descent," in *ICML*, 2005, pp. 89–96.
- [143] M. Collins and N. Duffy, "New ranking algorithms for parsing and tagging: Kernels over discrete structures, and the voted perceptron," in *ACL*, 2002, pp. 263–270.
- [144] R. Collobert and S. Bengio, "Links between perceptrons, mlps and svms," in *ICML*, 2004.
- [145] M. M. Bronstein, A. M. Bronstein, F. Michel, and N. Paragios, "Data fusion through cross-modality metric learning using similarity-sensitive hashing," in *CVPR*, 2010, pp. 3594–3601.
- [146] S. Kumar and R. Udupa, "Learning hash functions for cross-view similarity search," in *IJCAI*, 2011, pp. 1360–1365.
- [147] Y. Gong and S. Lazebnik, "Iterative quantization: A procrustean approach to learning binary codes," in *CVPR*, 2011, pp. 817–824.
- [148] Y. Zhen and D. Yeung, "Co-regularized hashing for multimodal data," in *NIPS*, 2012, pp. 1385–1393.
- [149] X. Zhu, Z. Huang, H. T. Shen, and X. Zhao, "Linear cross-modal hashing for efficient multimedia search," in *ACM Multimedia Conference, MM '13, Barcelona, Spain, October 21-25, 2013*, 2013, pp. 143–152.
- [150] D. Zhai, H. Chang, Y. Zhen, X. Liu, X. Chen, and W. Gao, "Parametric local multimodal hashing for cross-view similarity search," in *IJCAI*, 2013, pp. 2754–2760.
- [151] X. Liu, J. He, C. Deng, and B. Lang, "Collaborative hashing," in *CVPR*, 2014, pp. 2147–2154.
- [152] D. Zhang and W. Li, "Large-scale supervised multimodal hashing with semantic correlation maximization," in *AAAI*, 2014, pp. 2177–2183.
- [153] Z. Lin, G. Ding, M. Hu, and J. Wang, "Semantics-preserving hashing for cross-view retrieval," in *CVPR*, 2015, pp. 3864–3872.
- [154] Y. Zhen, Y. Gao, D. Yeung, H. Zha, and X. Li, "Spectral multimodal hashing and its application to multimedia retrieval," *IEEE Trans. Cybernetics*, vol. 46, no. 1, pp. 27–38, 2016.
- [155] G. Shakhnarovich, "Learning task-specific similarity," Ph.D. dissertation, Cambridge, MA, USA, 2005.
- [156] Y. Freund and R. E. Schapire, "A decision-theoretic generalization of on-line learning and an application to boosting," *J. Comput. Syst. Sci.*, vol. 55, no. 1, pp. 119–139, 1997.
- [157] Z. Yu, F. Wu, Y. Yang, Q. Tian, J. Luo, and Y. Zhuang, "Discriminative coupled dictionary hashing for fast cross-media retrieval," in *SIGIR*, 2014, pp. 395–404.
- [158] Y. Weiss, A. Torralba, and R. Fergus, "Spectral hashing," in *NIPS*, 2008, pp. 1753–1760.
- [159] W. Liu, J. Wang, S. Kumar, and S. Chang, "Hashing with graphs," in *ICML*, 2011, pp. 1–8.
- [160] J. Song, Y. Yang, Y. Yang, Z. Huang, and H. T. Shen, "Intermedia hashing for large-scale retrieval from heterogeneous data sources," in *SIGMOD*, 2013, pp. 785–796.
- [161] D. E. Rumelhart, J. L. McClelland, and C. PDP Research Group, Eds., *Parallel Distributed Processing: Explorations in the Microstructure of Cognition, Vol. 1: Foundations*. Cambridge, MA, USA: MIT Press, 1986.
- [162] G. E. Hinton and R. R. Salakhutdinov, "Replicated softmax: an undirected topic model," in *NIPS*, 2009, pp. 1607–1614.
- [163] J. Huang and B. Kingsbury, "Audio-visual deep learning for noise robust speech recognition," in *ICASSP*, 2013, pp. 7596–7599.
- [164] H. Hu, B. Liu, B. Wang, M. Liu, and X. Wang, "Multimodal dbn for predicting high-quality answers in cqa portals," in *ACL* (2), 2013, pp. 843–847.
- [165] L. Ge, J. Gao, X. Li, and A. Zhang, "Multi-source deep learning for information trustworthiness estimation," in *KDD*, 2013, pp. 766–774.
- [166] L. Pang and C.-W. Ngo, "Mutlimodal learning with deep boltzmann machine for emotion prediction in user generated videos," in *ACM ICMR*, 2015, pp. 619–622.
- [167] K. Sohn, W. Shang, and H. Lee, "Improved multimodal deep learning with variation of information," in *NIPS*, 2014, pp. 2141–2149.
- [168] M. Ehrlich, T. J. Shields, T. Almaev, and M. R. Amer, "Facial attributes classification using multi-task representation learning," in *CVPR Workshops*, 2016, pp. 47–55.
- [169] H. Larochelle and Y. Bengio, "Classification using discriminative restricted boltzmann machines," in *ICML*, 2008, pp. 536–543.
- [170] C. Hong, J. Yu, J. Wan, D. Tao, and M. Wang, "Multimodal deep autoencoder for human pose recovery," *IEEE Transactions on Image Processing*, vol. 24, no. 12, pp. 5659–5670, 2015.
- [171] B. S. Riggan, C. Reale, and N. M. Nasrabadi, "Coupled auto-associative neural networks for heterogeneous face recognition," *IEEE Access*, vol. 3, pp. 1620–1632, 2015.
- [172] H. Amiri, P. Resnik, J. Boyd-Graber, and H. D. III, "Learning text pair similarity with context-sensitive autoencoders," 2016.
- [173] H. Lee, C. Ekanadham, and A. Y. Ng, "Sparse deep belief net model for visual area v2," in *NIPS*, 2008, pp. 873–880.
- [174] C. Silberer and M. Lapata, "Learning grounded meaning representations with autoencoders," in *ACL (1)*, 2014, pp. 721–732.
- [175] W. Wang, B. C. Ooi, X. Yang, D. Zhang, and Y. Zhuang, "Effective multi-modal retrieval based on stacked auto-encoders," *Proceedings of the VLDB Endowment*, vol. 7, no. 8, pp. 649–660, 2014.
- [176] S. Rastegar, M. Soleymani, H. R. Rabiee, and S. Mohsen Shoaiee, "Mdl-cw: A multimodal deep learning framework with cross weights," in *CVPR*, 2016, pp. 2601–2609.
- [177] A. Frome, G. S. Corrado, J. Shlens, S. Bengio, J. Dean,

and T. Mikolov, "Devise: A deep visual-semantic embedding model," in *NIPS*, 2013, pp. 2121–2129.

[178] P. Huang, X. He, J. Gao, L. Deng, A. Acero, and L. P. Heck, "Learning deep structured semantic models for web search using clickthrough data," in *CIKM*, 2013, pp. 2333–2338.

[179] A. M. Elkahky, Y. Song, and X. He, "A multi-view deep learning approach for cross domain user modeling in recommendation systems," in *WWW*, 2015, pp. 278–288.

[180] J. Dong, X. Li, and C. G. Snoek, "Word2visualvec: Cross-media retrieval by visual feature prediction," *arXiv preprint arXiv:1604.06838*, 2016.

[181] R. Kiros, R. Salakhutdinov, and R. S. Zemel, "Multimodal neural language models," in *ICML*, vol. 14, 2014, pp. 595–603.

[182] A. Lazaridou, N. T. Pham, and M. Baroni, "Combining language and vision with a multimodal skip-gram model," *arXiv preprint arXiv:1501.02598*, 2015.

[183] T. Mikolov, K. Chen, G. Corrado, and J. Dean, "Efficient estimation of word representations in vector space," *arXiv preprint arXiv:1301.3781*, 2013.

[184] J. Dean, G. Corrado, R. Monga, K. Chen, M. Devin, M. Mao, A. Senior, P. Tucker, K. Yang, Q. V. Le *et al.*, "Large scale distributed deep networks," in *NIPS*, 2012, pp. 1223–1231.

[185] M. Norouzi, T. Mikolov, S. Bengio, Y. Singer, J. Shlens, A. Frome, G. S. Corrado, and J. Dean, "Zero-shot learning by convex combination of semantic embeddings," *arXiv preprint arXiv:1312.5650*, 2013.

[186] H. Fang, S. Gupta, F. Iandola, R. K. Srivastava, L. Deng, P. Dollár, J. Gao, X. He, M. Mitchell, J. C. Platt *et al.*, "From captions to visual concepts and back," in *CVPR*, 2015, pp. 1473–1482.

[187] Y. Feng and M. Lapata, "Visual information in semantic representation," in *HLT-NAACL*, 2010, pp. 91–99.

[188] E. Bruni, N.-K. Tran, and M. Baroni, "Multimodal distributional semantics," *J. Artif. Intell. Res.(JAIR)*, vol. 49, no. 1–47, 2014.

[189] D. Kiela and L. Bottou, "Learning image embeddings using convolutional neural networks for improved multi-modal semantics," in *EMNLP*, 2014, pp. 36–45.

[190] W. Yih, X. He, and C. Meek, "Semantic parsing for single-relation question answering," in *ACL*, 2014, pp. 643–648.

[191] R. Xu, C. Xiong, W. Chen, and J. J. Corso, "Jointly modeling deep video and compositional text to bridge vision and language in a unified framework," in *AAAI*, 2015, pp. 2346–2352.

[192] T. Mikolov, M. Karafiat, L. Burget, J. Cernocky, and S. Khudanpur, "Recurrent neural network based language model," in *Interspeech*, vol. 2, 2010, p. 3.

[193] S. Hochreiter and J. Schmidhuber, "Long short-term memory," *Neural Comput.*, vol. 9, no. 8, pp. 1735–1780, Nov. 1997.

[194] K. Cho, B. van Merriënboer, Ç. Gülcehre, D. Bahdanau, F. Bougares, H. Schwenk, and Y. Bengio, "Learning phrase representations using RNN encoder-decoder for statistical machine translation," in *EMNLP*, 2014, pp. 1724–1734.

[195] I. Sutskever, O. Vinyals, and Q. V. Le, "Sequence to sequence learning with neural networks," in *NIPS*, 2014, pp. 3104–3112.

[196] Y. Bengio, P. Simard, and P. Frasconi, "Learning long-term dependencies with gradient descent is difficult," *IEEE Transactions on Neural Networks*, vol. 5, no. 2, pp. 157–166, 1994.

[197] R. Kiros, R. Salakhutdinov, and R. S. Zemel, "Unifying visual-semantic embeddings with multimodal neural language models," *arXiv preprint arXiv:1411.2539*, 2014.

[198] S. Venugopalan, H. Xu, J. Donahue, M. Rohrbach, R. Mooney, and K. Saenko, "Translating videos to natural language using deep recurrent neural networks," *arXiv preprint arXiv:1412.4729*, 2014.

[199] S. Venugopalan, M. Rohrbach, J. Donahue, R. Mooney, T. Darrell, and K. Saenko, "Sequence to sequence-video to text," in *ICCV*, 2015, pp. 4534–4542.

[200] S. Antol, A. Agrawal, J. Lu, M. Mitchell, D. Batra, C. Lawrence Zitnick, and D. Parikh, "Vqa: Visual question answering," in *ICCV*, 2015, pp. 2425–2433.

[201] H. Palangi, L. Deng, Y. Shen, J. Gao, X. He, J. Chen, X. Song, and R. K. Ward, "Deep sentence embedding using long short-term memory networks: Analysis and application to information retrieval," *IEEE/ACM Trans. Audio, Speech & Language Processing*, vol. 24, no. 4, pp. 694–707, 2016.

[202] X. Chen and C. L. Zitnick, "Learning a recurrent visual representation for image caption generation," *arXiv preprint arXiv:1411.5654*, 2014.

[203] D. Bahdanau, K. Cho, and Y. Bengio, "Neural machine translation by jointly learning to align and translate," *CoRR*, vol. abs/1409.0473, 2014.

[204] J. Ba, V. Mnih, and K. Kavukcuoglu, "Multiple object recognition with visual attention," *CoRR*, vol. abs/1412.7755, 2014.

[205] V. Mnih, N. Heess, A. Graves, and K. Kavukcuoglu, "Recurrent models of visual attention," *CoRR*, vol. abs/1406.6247, 2014.

[206] D. Zhou, J. Weston, A. Gretton, O. Bousquet, and B. Schölkopf, "Ranking on data manifolds," in *NIPS*, 2003, pp. 169–176.

[207] X. Mao, B. Lin, D. Cai, X. He, and J. Pei, "Parallel field alignment for cross media retrieval," in *ACM Multimedia*, 2013, pp. 897–906.

PLACE
PHOTO
HERE

Yingming Li received the BS and MS degrees in automation from University of Science and Technology of China, Hefei, China, and the PhD degree in information science and electronic engineering from Zhejiang University, Hangzhou, China. He is currently an assistant professor with the College of Information Science and Electronic Engineering at Zhejiang University, China.

PLACE
PHOTO
HERE

Ming Yang received the BS, MS, and PhD degrees in information science and electronic engineering from Zhejiang University, Hangzhou, China. He had been a visiting scholar in computer science at the State University of New York (SUNY) at Binghamton.

PLACE
PHOTO
HERE

Zhongfei (Mark) Zhang received the BS degree in electronics engineering, the MS degree in information science, both from Zhejiang University, Hangzhou, China, and the PhD degree in computer science from the University of Massachusetts at Amherst. He is a QiuShi Chaired Professor at Zhejiang University, China, and directs the Data Science and Engineering Research Center at the university while he is on leave from State University of New York (SUNY) at Binghamton, USA, where he is a professor at the Computer Science Department and directs the Multimedia Research Laboratory in the Department. He has published more than 200 peer-reviewed academic papers in leading international journals and conferences and several invited papers and book chapters, has authored or co-authored two monographs on multimedia data mining and relational data clustering, respectively.